

University of Nevada, Reno

Photo-Activation of 2,2'-Bipyridine-Sulfur Oxides Donor-Acceptor Complex

A thesis submitted in partial fulfillment of the requirements

For the degree of Master of Science in

Chemistry

by

Connor J. Filbin

Dr. Ying Yang/Thesis Advisor

May 2022

Copyright by Connor J. Filbin 2022 All Rights Reserved



THE GRADUATE SCHOOL

We recommend that the thesis
prepared under our supervision by

CONNOR J. FILBIN

entitled

**Photo-Activation of 2,2'-Bipyridine-Sulfur
Oxides Donor-Acceptor Complex**

be accepted in partial fulfillment of the
requirements for the degree of

MASTER OF SCIENCE

Ying Yang, Ph.D.
Advisor

Matthew J. Tucker, Ph.D.
Committee Member

Xiaoshan Zhu, Ph.D.
Graduate School Representative

David W. Zeh, Ph.D., Dean
Graduate School

May, 2022

Abstract

The work presented in this thesis discusses the synthesis of a novel photochromic molecule which is induced by a bipyridine-sulfur dioxide (SO_2) charge transfer mechanism. SO_2 is produced in large quantities by many industrial processes, and great effort is spent to reduce its emission. SO_2 is an underutilized feedstock for chemical reactions and functional materials alike, so great interest is applied to new uses of this byproduct.

Photochromic bipyridines typically appear N, N'-disubstituted-4,4'-bipyridines, known as viologens. Following exposure to UV light, viologens undergo a one electron reduction to a blue colored radical cation. This radical cation is easily detectable by EPR spectroscopy. The photochromic bipyridine presented in this work undergoes a color change from light yellow to magenta upon irradiation, resulting in a new absorption peak at 550 nm. The EPR spectroscopy of the irradiated colored product does not detect any radicals, which suggests a new mechanism different from viologens.

The present bipyridine containing system exhibits photochromic response for small molecule solids, small molecule solutions, and polymeric systems. Each of these environments exhibit tunable color change. Small molecule solutions and polymeric systems exhibit t-type photochromic behavior. DFT calculations were performed on the photochromic small molecule complexed with SO_2 . The results of these calculations indicate that photochromism is attributed to a UV-induced bipyridine- SO_2 bond strengthening. The decrease of N-S bond length lowers the energy of the charge transfer band into the visible range. This represents a new class of photo-responsivity which can be applied to various applications common to photo switching materials. The

concluding remarks suggest future directions of mechanistic studies as well as implementation of the photoproduct in film fabrication, and as a light induced mechano-responsive material.

Acknowledgements

This research was funded by the University of Nevada, Reno start-up fund. I would like to acknowledge the guidance and training by Dr. Stephen Spain and Dr. Nina Ruprecht for instruments used in the shared instrument lab. I would like to thank my group members Dr. Lasith Kariyawasam, Cameron Locke, Ryan Meehan, Chao Wang, and Julian Rolsma for indispensable guidance within the lab. Finally, I'd like to thank Dr. Ying Yang, not only for all she has taught me over the years, but for instilling confidence within me to pursue a graduate education, which ultimately led to me finding my passion in life.

3.4 Irradiation dependance on viscosity.....	35
3.5 Summary of Findings.....	36
Chapter 4. Conclusion and Outlook.....	37
4.1 Conclusions.....	37
4.2 Outlook	37
Conflicts of interest.....	39
References.....	40

List of Figures

Figure 1. Photochromic response of 2,2'-bipyridine-4,4'-diester products of synthesis route a and b in their deprotonated states (**1a** and **1b**) and their protonated states (**1a-H⁺** and **1b-H⁺**)

Figure 2. The NMR spectra which shows the structural similarity of the two synthetic routes (A) through acid chloride intermediate and (B) through Fischer esterification.

Figure 3. ATR spectrum of 1a (blue line) vs 1b (red line) of spectra showing (A) comparison at 1340 cm^{-1} signifying a lack of free SO_2 . (B) two new peaks appear at 1020 and 900 cm^{-1} which signify new binding modes in the presence of sulfur oxides

Figure 4. EPR spectra of methyl viologen before irradiation (black line) after irradiation (red line) and after heating the irradiated product at $60\text{ }^\circ\text{C}$ for 15 mins (blue line).

Figure 5. EPR spectra before and after irradiation of the solid A) **1a-H⁺** without the presence of any radicles and B) **1b-H⁺** shows the presence of a small radicle concentration

Figure 6. Powder XRD for 1a-H⁺ before irradiation (black solid line) vs irradiated 1a-H⁺ (red dashed line)

Figure 7. Irradiation of 1a-H⁺ with various wavelengths of visible light. Irradiation with 395 and 470 nm (blue) light induced significant color change while 520 nm (green) light induced slight color change to pink. Irradiation with 630 nm (red) light was unsuccessful at inducing color change.

Figure 8. (A) Reversible color change of 20 mM **1a-H⁺** dissolved in CHCl_3 :TEGMME 50:50 and its (B) absorption spectra under timed 395 nm irradiation. (C) Cyclability of photochromic response after heating for 4 minutes under $75\text{ }^\circ\text{C}$ followed by 20 minutes of irradiation. (D) Decay of color after irradiated solution is left in dark storage over time

Figure 9. Photochromic response of 1a-H⁺ dissolved in CHCl_3 :TEGDME 50:50 under timed 395 nm irradiation for a A) 20 mM solution and B) 80 mM solution.

Figure 10. UV-vis absorption spectra of 80 mM 2,2'-bipyridine (black line), 20 mM bpy-dBu(a) (red line), bpyH⁺-dBu(a) (blue line), bpy-dBu(b) (green line), bpyH⁺-dBu (purple line) after 5 minutes of SO_2 bubbling in 50:50 CHCl_3 :TEGMME

Figure 11. A) Equilibrium between the protonated bipyridyl and bipyridine- SO_2 complex. B) ^1H NMR shifts for a) non-irradiated **1a-H⁺**, b) **1a-H⁺** after SO_2 bubbling in CDCl_3 , and c) **1a-H⁺** irradiated with 395 nm light for 20 min in the solid state and then dissolved in CDCl_3 for data collection.

Figure 12. ^1H NMR shifts before and after 30 min irradiation at 395 nm for 1b-H⁺ indicate a smaller loss of HCl upon irradiation for products that have never been exposed to SO_2 .

Figure 13. (A) A positive linear relationship between excitation wavelength and emission wavelength for 1a-H⁺ solutions containing TEGMME:CHCl₃ 1:1. (B) The emission of 454 nm light following 395 nm excitation (red point) is the highest intensity compared emissions induced by other excitation wavelengths.

Figure 14. Structures and potential energy surfaces of **2a-2c** obtained at the B3LYP-D3BJ/def2-TZVP level. Structure 2a (black line) 2b-trans (blue line), and 2c (pink line) exhibit no unique features representative of a photochromic response, while 2b-cis (red line) shows a local energetic minimum at a decreased bond length

Figure 15. Calculated spectra of non-equilibrium structures of 2a-2c formed after photoirradiation. Spectra are convoluted with Lorentzian functions with FWHM of 4 nm. Spectra of 2b-cis conformations of N-S bond distances 1.475 Angs. (green) and 1.662 Angs. (red) contain absorbances between 500-550 nm, consistent with experimental results.

Figure 16. 2,2'-bipyridine-4,4' diester functionalized polyethylene glycol 2000 g/mol polymers showing stable photo-responses after irradiation, thermal treatment, and dark storage.

Figure 17. Photochromic response of 2,2'-bipyridine-4,4'-diester polymeric samples of type PEG 300 (1), PEG 4000 (2), PPG 425 (3), PPG 4000 (4)

Figure 18. Viscosity response of 2,2'-bipyridine 4,4'-diester containing polyethylene glycol 300 g/mol in the irradiated and non-irradiated stat

List of Schemes

Scheme 1. Synthesis of the 2,2'-bipyridine-4,4' diester derivatives through acid chloride intermediate (route a) and Fischer esterification (route b).

Chapter 1. Introduction

1.1 Photochemistry

Before the advent of modern spectroscopic techniques, chemists relied on color change to signify chemical change. Predictably, color change inspired the first report of a photochemical reaction. In 1834, Trommsdorff described a white crystal color changing to yellow upon exposure to sunlight, continued exposure caused the crystal to explode.¹ This shocking result interested chemists for generations, yet took over 170 years for the mechanism of this reaction to be entirely understood.² The difficulty to determine its mechanism stems from the unpredictability of the core component of a photochemical reaction: the excited state electron. A ground state electron resting in a bonding or nonbonding orbital is promoted to an excited state antibonding orbital following the exposure of a high energy wavelength of light. This wavelength of light falls within the range of ultraviolet or visible light for most organic compounds. All molecules experience these electronic transitions, yet not all transitions can result in significant molecular transformations. In select systems, an excited state electron can overcome an energy barrier that is too steep (or does not exist) in the ground state, to afford a product that is thermally forbidden. When these systems arise, it is important to study their mechanism for possible use in functional materials. Photoresponsive molecules are essential building blocks in functional materials for data storage, optoelectronic devices, controlled assembly and release, catalysis, sensing, and actuating.³⁻⁸ Modern photochemistry has determined four major photochemically allowed pathways induced by excited state electrons: isomerization, bond cleavage, bond formation, and molecular rearrangements.⁴ Photochromic molecules utilizing these pathways are of great interest as of recent.

Photochromic molecules, following absorption of high energy ultraviolet light, form a photoproduct that changes its absorbance into the visible range.⁵ When a molecule absorbs light in the visible range our eyes perceive it as colored. The color of the product appears as the wavelength of visible light complementary to the absorbed light.⁹ The colored photoproduct is reversible back to the original isomer through exposure to a different wavelength of light, or thermal treatment. Photochromic molecules which are reversible by light exposure are known as ‘p-type’ while those reversible by thermal treatment are known as ‘t-type’. Derivatives of azobenzene¹⁰, spiropyran¹¹, diarylethane¹², and viologens¹³ are four of the most widely used photochromic molecules. Azobenzene, upon ultraviolet irradiation, undergoes an isomerization of a N=N bond from a planar trans isomer to a bent cis isomer. UV irradiation of spiropyran initiates an electrocyclic ring opening reaction which increases conjugation allowing for absorption in the visible range. Conversely, diarylethanes undergo a UV induced ring closing mechanism. Finally, N,N'-di-quaternized bipyridyl salts, also known as viologens, exhibit reversible photochromism under ultraviolet light through redox reactions. One electron reduction of a bipyridinium to the colored radical cation can occur electrochemically or by UV irradiation. In this study, we report a new photochemical pathway that involves dynamic interactions between 2,2'-bipyridine derivatives and sulfur dioxide (SO₂).

1.2 The SO₂ problem and opportunities

Millions of tons of SO₂ are produced as a byproduct of coal-fired power plants, smelting mineral ores, and volcanic eruptions.¹⁴⁻¹⁶ Scrubbing SO₂ is an expensive, but

necessary process to reduce emissions.¹⁷ Only a few industrial processes use SO₂ as a feedstock, those include the production of sulfuric acid, paper, and food preservation.¹⁸ In the pharmaceutical industry, products containing sulfonyl groups (-SO₂-) have been reported for haemorrhoid treatment.¹⁹ Current functional materials focus on SO₂ sensing rather than using the gas as a driving force for dynamic response.²⁰⁻²² The use of SO₂ as a reagent for chemical synthesis is uncommon due to the complexity of handling the toxic gas. Pioneering work by Willis et. al demonstrates a technique for molecular insertion of SO₂ through the use of a bis-SO₂ surrogate.^{23,24} Although these advancements have been made, widespread use of SO₂ complexes in functional materials is lacking. The challenge for these compounds results from traditionally weak interaction between SO₂ and ligands such as amines.²⁵ In addition to their weak interactions, they are also often air sensitive. The present work utilizes SO₂ to play an integral role in a novel functional material which is stable under ambient conditions.

1.3 SO₂-amine interactions

2,2'-bipyridine is one of the most widely used ligands.²⁶ This is due to 2,2'-bipyridine being a neutral bidentate ligand that is redox stable and easy to functionalize. A donor-acceptor interaction occurs through donation of available electrons residing in highest occupied molecular orbital (HOMO) of a Lewis base, to the lowest unoccupied molecular orbital (LUMO) of a Lewis acid. When these orbitals are sufficiently aligned a charge transfer event can occur. The complexes formed between donor and acceptor are known as charge-transfer complexes. Due to orbital mixing, a charge transfer complex's orbitals are more stabilized than that of its individual components. In metal coordination

chemistry, 2,2'-bipyridine is the electron rich Lewis base whose sp^2 lone pair electrons are donated to the electron deficient d-orbitals of Lewis acid transition metals. Metal to ligand charge transfer complexes, upon complexation, result in a myriad of vibrantly colored species.²⁷⁻³⁰ In this case, orbital mixing decreases the HOMO-LUMO gap significantly enough to where low energy visible light absorption occurs. The absorbance indicative of the electron transfer is known as the charge-transfer band. The present study considers a donor-acceptor interaction that instead utilizes a plentiful pollutant, SO_2 , as the Lewis acid.

The donor-acceptor complex between SO_2 and amines is a long-known chemistry.³¹ Except for tertiary amines with sp^3 hybridized N atoms, most amines interact weakly with SO_2 . It has been reported that SO_2 forms colored charge transfer complexes with aromatic amines such as N,N'-dimethylaniline and N,N'-diethylaniline.^{32,33} The HOMO is localized in the aromatic amine non-bonding lone pair and LUMO is in SO_2 antibonding p orbitals. Despite the long-history since the discovery of SO_2 -amine complexes, their photosensitivity has not yet been reported. Herein, we demonstrate the photochromism of simple 2,2'-bipyridine derivatives and the corresponding polymers enabled by sulfur dioxide (SO_2). They change from yellow and magenta when irradiated with UV light and relax back to the yellow form in the dark with good cyclability. Different from the well-known viologens, free radicals were absent in the photoactivated colored product even when the bipyridines are protonated. We also found that when 2,2'-bipyridines are incorporated in solid polyethylene glycols (PEG), the thermally stable yellow form and photoactivated magenta form both remain stable at room temperature, representing a unique photo-switching behavior.

1.4 Overview of this study

The origin of this work stems from an observation following the synthesis of bipyridine containing polymers for use in a metallosupramolecular network. The polymer, which was a low molecular weight 2,2'-bipyridine functionalized with polyethylene glycol at the 4,4'- positions, appeared as a yellow color viscous fluid as synthesized. Storage of the product in a drawer for an indefinite amount of time showed no change to the initial yellow color. However, when the product was left out on the bench in direct sunlight the product quickly changed to an orange-colored liquid then later to a red-wine colored liquid. The photoproduct was able to return to the initial yellow color after minutes of 75 °C thermal treatment. The photo response of this liquid was found to be repeatable over many repeated syntheses of the same product, so we sought to investigate its mechanism. It quickly proved difficult to spectroscopically analyze the polymeric product for changes between the yellow and red colored state. This is primarily due to the decreased resolution of the bipyridine peaks in the presence of a high molecular weight backbone. As a result, a small molecule exhibiting the same photochromic response was developed.

This work presents a successful synthesis of a novel photochromic molecule utilizing a 2,2'-bipyridine and sulfur oxides interaction as the chromophore. The photoactivated mechanism was investigated. The photochromic small molecule was then functionalized with various polymeric backbones which afforded unique photo responses depending on molecular weight and backbone character.

1.5 Organization of this work

Chapter 1 introduces the photoreactions, examples of common photochromic molecules, relevance of SO₂ functional materials, and pyridine-SO₂ interactions previously discussed in literature. Chapter 2 analyzes the photochromic small molecule in both solid and solution state for mechanistic insights, then discusses the simulation data conducted by Dr. Samuel Odoh's group and its agreement to experimental results. Chapter 3 presents the characteristics of polymeric products functionalized with the chromophore. Chapter 4 summarizes the principal findings and suggests directions of future studies.

Chapter 2. Photochromism of 2,2'-Bipyridine Small Molecule Derivatives

2.1 Introduction

Photochromic bipyridines exclusively exists in literature as N,N'-di-quaternized bipyridyl salts, commonly known as viologens.³⁴ Upon 395 nm ultra violet (UV) irradiation, these white crystalline molecules undergo a one electron reduction to a radical cation, which appears blue in color.^{35,36} Due to the presence of a radical, this mechanism can be easily identified through electron paramagnetic resonance (EPR) spectroscopy. Following the synthesis of a simple 2,2'-bipyridine-4,4'-dibutyl ester it was noticed that 395 nm irradiation resulted in a color change from yellow to pink. EPR spectroscopy of the colored form indicated no presence of a radical; therefore, a new mechanism should be considered for this molecule.

First, variation of synthetic route determined the photoresponsivity was a result of interactions with reaction byproducts rather than a property unique to the isolated molecule. When 2,2'-bipyridine-4,4'-dibutyl ester was formed through an acid chloride immediate

photochromic response was observed, while the same target molecule formed by Fischer esterification was non photochromic. We then developed a unique solvent system where reversible photochromic response is observed. The highest intensity peaks within the visible range were present after 20 minutes of irradiation. The color decayed following thermal treatment or dark storage. The reversible photochromic response was shown to have consistent cyclability with limited color fatigue. To isolate the role of SO₂ in the photochromic molecule, solutions containing the 2,2'-bipyridine-4,4'-dibutyl ester of both synthetic routes were directly exposed to SO₂ gas in the dark. The resulting UV visible spectra yielded identical spectra as the photochromic solutions. Finally, collaboration with Dr. Samuel Odoh revealed the preferred complexation orientation between bipyridine and SO₂ as a 1:1 cis conformation. Furthermore, this complexation demonstrated DFT calculated absorbances consistent with experimental results.

2.2 Experimental

2.2.1. Synthesis of 2,2'-bipyridine-4,4'-dibutyl ester from acid chloride (route a) (1a)

2,2'-bipyridine-4,4'-dicarboxylic acid (0.637 g, 2.62 mmol), 10 mL of thionyl chloride, and 100 μ L pyridine was added to a 50 mL round bottom flask, and the mixture was refluxed for 48 hours in N₂ atmosphere. The yellow-colored 2,2'-bipyridine-4,4'-diacid chloride solution was heated under reduced pressure to remove thionyl chloride. Then for two iterations, chloroform was added to the yellow solid and subsequently removed under reduced pressure. The acid chloride intermediate was dissolved in 3 mL chloroform. 1-butanol (0.790 g, 10.7 mmol) was dissolved in 2 mL chloroform and added dropwise into the acid chloride solution followed by the addition of 200 μ L pyridine. The

mixture was stirred at room temperature for 18 hours in N₂ atmosphere. 0.5 g of potassium carbonate was added to the mixture and stirred at room temperature for 18 hours. The solution was then filtered from the insoluble potassium carbonate and added dropwise into 15 mL deionized water. The organic layer was removed and added dropwise into a fresh 15 mL aliquot of deionized water for two more iterations. The organic layer was removed and initially dried by rotary evaporation, then overnight in the vacuum oven at 45 °C. Yield of pink colored solid is 79% (0.736 g, 2.06 mmol). ¹H NMR (400 MHz, cdcl₃) δ 8.94 (d, *J* = 1.5 Hz, 1H), 8.87 (d, *J* = 5.0 Hz, 1H), 7.91 (dd, *J* = 5.0, 1.6 Hz, 1H), 4.41 (t, *J* = 6.7 Hz, 2H), 1.86 – 1.75 (m, 2H), 1.57 – 1.41 (m, 2H), 1.00 (t, *J* = 7.4 Hz, 3H).

2.2.2. Fischer esterification of 2,2'-bipyridine-4,4'-dibutyl ester (route b) (1b)

2,2'-bipyridine 4,4'-dicarboxylic acid (0.2657 g, 1.09 mmol), 8 mL 1-butanol, and 800 μL H₂SO₄ was added to a 25 mL round bottom flask and the mixture was refluxed for 3 hours. After the solution was cooled to room temperature, the mixture was added to cold deionized water which immediately formed a light pink precipitate. The precipitate was collected by filtration and washed with distilled water and methanol. Upon washing with methanol, the pink precipitate became white. The product was dried under vacuum at room temperature. Yield of white powdered product 72% (0.282 g, 0.791 mmol). ¹H NMR (400 MHz, cdcl₃) δ 8.97 – 8.90 (m, 1H), 8.87 (ddd, *J* = 5.0, 0.9, 0.4 Hz, 1H), 7.99 – 7.87 (m, 1H), 4.41 (td, *J* = 6.7, 0.9 Hz, 2H), 1.87 – 1.75 (m, 2H), 1.66 – 1.33 (m, 2H), 1.05 – 0.88 (m, 3H)

2.2.3. Protonation procedure

Concentrated HCl solution was added into a three-neck round bottom flask. A N₂ gas line was submerged into the HCl solution. Purified charge neutral products (routes a and b) were added to separate vial and dissolved in chloroform. A second line exiting the three-neck flask is submerged into the chloroform solution. This line captures N₂ gas carrying HCl vapor. N₂ flows through the system for a total of 60 seconds. Chloroform is removed by rotary evaporation, and dried under vacuum at 45 °C, affording a yellow-colored product.

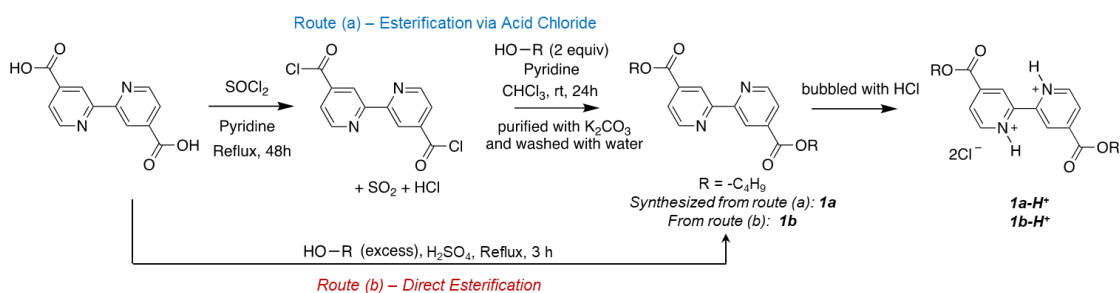
2.2.4. Characterization and methods

¹H NMR spectra were recorded on a 400 MHz or 500 MHz Varian NMR spectrometer using CDCl₃ as solvent. The chemical shifts are reported with respect to TMS ($\delta(1H) = 0.00$ ppm). UV-visible spectra were recorded on a Shimadzu UV 2550 spectrometer. EPR spectra were recorded on a Bruker EMXPlus EPR at room temperature. Fluorescence spectra were recorded on a Jobin Yvon Horiba FluoroMax-3. Attenuate Total Reflection Fourier-transform infrared spectroscopy (ATR-FTIR) was collected using a Thermo Nexus 470 FT-IR with ZeSe and Ge ATR at room temperature under ambient conditions over the range of 650 to 4000 cm⁻¹. Powder X-ray diffraction (PXRD) spectra were recorded on Bruker D2 X-ray diffractometer. X-rays sourced from Cu K α radiation ($\lambda = 1.5406$ Å) over the range of $4^\circ < 2(\theta) < 60^\circ$ in 0.02° steps measurements with a scan rate of 1°/min. Solid state samples were loaded on a zero-diffraction silicon wafer coated with a thin layer of vacuum grease.

2.3. Results and discussion

2.3.1 Solid state color change

A 2,2'-bipyridine functionalized with ester groups at the 4,4'- position was observed to be photochromic. A 2,2'-bipyridine-4,4'-dicarboxylic acid, in the presence of thionyl chloride, was converted into an acyl chloride intermediate. Addition of pyridine, to remove acid protons, and two molar equivalents of 1-butanol formed a 2,2'-bipyridine-4,4'-dibutyl ester (**1a**) (Scheme 1, route a). The yellow-colored crude product exhibited a color change to magenta within minutes following exposure to 395 nm ultraviolet light (UV).



Scheme 1. Synthesis of the 2,2'-bipyridine-4,4' diester derivatives through acid chloride intermediate (route a) and Fischer esterification (route b).

At this stage it was unclear whether pyridine was involved in the photochromic mechanism, as aromatic stacking compounds are also reported to be photochromic.³⁷ Therefore removal of pyridine was necessary to see if photochromism was still present in its absence.

In the reaction, pyridine acts as a base which binds with acidic protons released during the esterification. However, since the esterification occurred on a bipyridine moiety, which is also basic, pyridine and bipyridine compete for acidic hydrogens resulting in both being protonated. Pyridine's conjugate acid, pyridinium, has a pK_a of 5.2, while the

bipyridinium has a pK_{a1} of 4.4.^{38,39} Bipyridinium and pyridinium also have similar solubilities, which are, in turn, difficult to separate. Deprotonation with potassium carbonate regenerates pyridine and bipyridine, which now have unique solubilities. Pyridine is then washed away in an aqueous layer while the bipyridine product stays in the organic layer which can be separated.

After purification, the deprotonated **1a** was magenta colored and remained unchanged after prolonged irradiation. However, after reprotonation by hydrochloric acid (HCl) bubbling, **1a-H⁺** was once again yellow colored and photochromism was reinstated (Fig. 1).

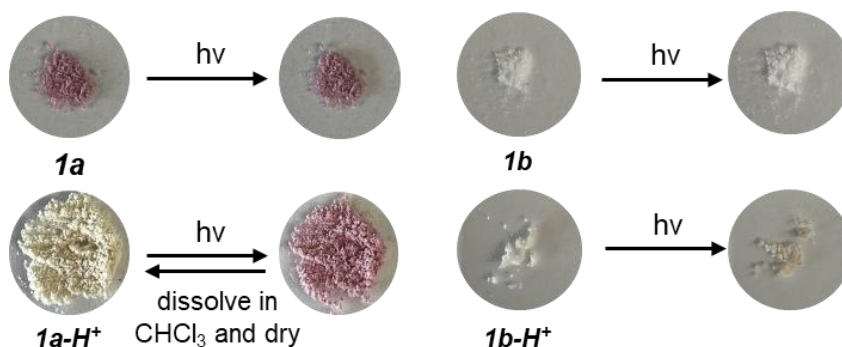


Figure 1. Photochromic response of 2,2'-bipyridine-4,4'-diester products of synthesis route a and b in their deprotonated states (**1a** and **1b**) and their protonated states (**1a-H⁺** and **1b-H⁺**)

While in the solid state, the photochromic response of **1a-H⁺** is stable in the dark and at elevated temperatures. Reversibility to the yellow product was shown through additional reprotonation by HCl bubbling or dissolution in CHCl_3 followed by drying. The re-processed compound, upon UV irradiation, can readily color change to pink.

To identify if the photochromic response is controlled by the synthetic route, the same 2,2'-bipyridine-4,4'-diester compound was now synthesized by Fischer esterification catalyzed by sulfuric acid (Scheme 1, route b). The resulting product after purification, **1b**,

appears identical to the purified product **1a** through NMR analysis (Fig. 2). Pure **1b** exists as a white powder which did not color change following 30 minute of 395 nm irradiation. After HCl bubbling, the protonated **1b-H⁺** still appeared as a white solid which changed to yellow after 30 minutes of 395 nm irradiation (Fig. 1). Here it can be concluded that the color change from yellow to pink is exclusive to the acid chloride intermediate synthetic route. Sulfur dioxide (SO₂) is produced as a byproduct of the conversion from carboxylic acid to acid chloride in the presence of thionyl chloride. Due to this, we hypothesize SO₂ drives the photochromic response.

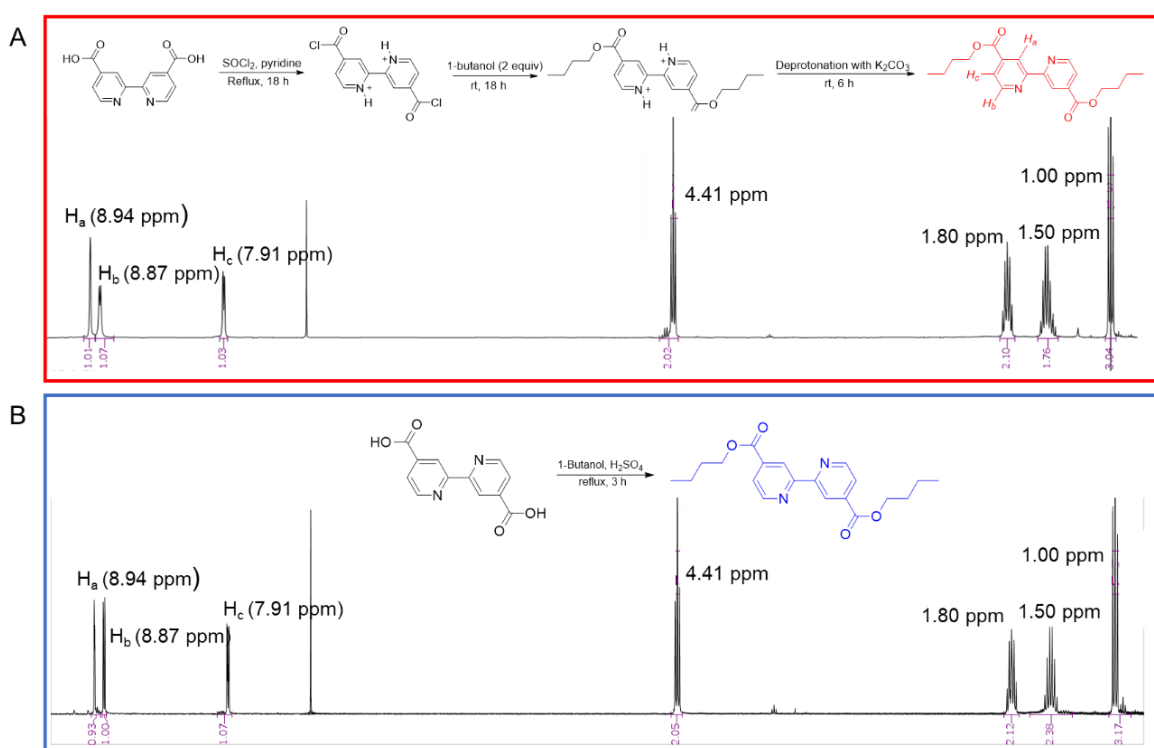


Figure 2. The NMR spectra which show the structural similarity of the two synthetic routes (A) through acid chloride and (B) through Fischer esterification.

ATR-FTIR analysis of the solid-state products **1a** and **1b** was expected show the existence of SO₂ or the oxidized sulfur trioxide (SO₃) if there is any in the solid state. **1a** has been exposed to SO₂ during the acid chloride intermediate synthesis while **1b** was synthesized without any presence of SO₂. The S=O stretching vibrations of SO₂ and SO₃

usually absorb in the region of 1300-1350 cm^{-1} .⁴⁰ When comparing the charge neutral product's spectrums, there does not exist additional peaks in this region in **1a** compared to **1b** (Fig. 3A). However, two new peaks do appear at 1020 and 900 cm^{-1} in **1a** (Fig. 3B). When comparing the spectra of **1a** to non-irradiated **1a-H⁺** these peaks are also present to the same intensity. This eliminates the possibility of either of the modes being assigned to an N-S interaction as the acidic proton of **1a-H⁺** would occupy the nitrogen binding site. Further analysis is necessary to accurately assign these modes. Residual amounts of sulfur oxides below the detection limit of the FTIR may be present in the products.

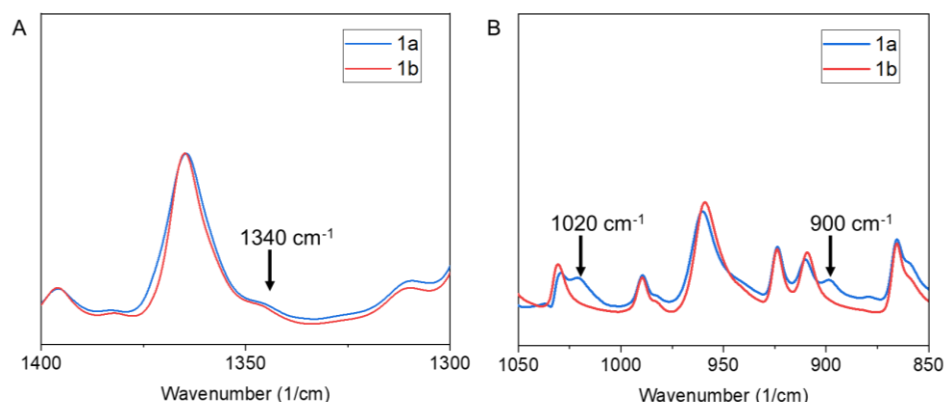


Figure 3. ATR-FTIR spectra of **1a** (blue line) and **1b** (red line) showing that (A) comparison at 1340 cm^{-1} signifying a lack of free SO_2 , and (B) two new peaks appear at 1020 and 900 cm^{-1} which signify new binding modes in the presence of sulfur oxides

Before considering a new mechanism, the present photochromic molecule must be compared to the mechanism of the well-known viologen. Viologens, following 395 nm irradiation, undergo a one electron reduction to form a blue colored radical cation. The radical cation is reversible with heat back to the colorless form. As a control, we performed EPR spectroscopy at room temperature on a commercially available dimethyl viologen solid (Fig. 4). The nonirradiated methyl viologen did not respond to EPR after sweeping

through the organic radicle region between 3200 and 3500 Gauss. After 15 minutes irradiation with 395 nm light the viologen turned colored, and the EPR presented a significant derivative peak attributed to the radicle cation. Heating for 15 minutes at 60 °C lightened the viologen's color and showed the decrease of the derivative peak, thereby the decrease of the radicle cation concentration.

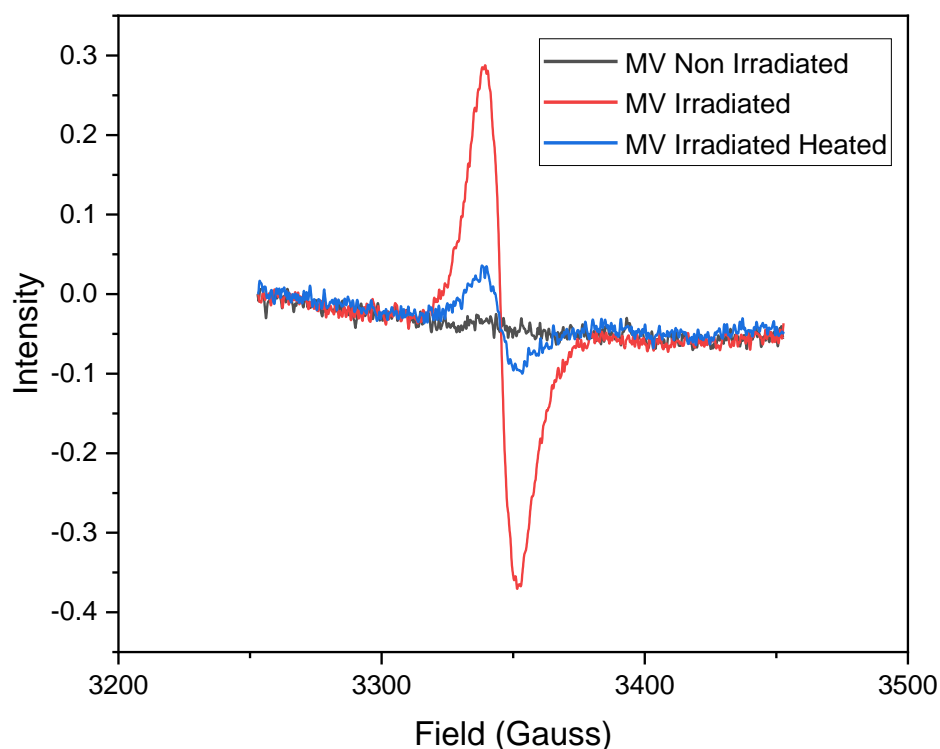


Figure 4. EPR spectra of methyl viologen before irradiation (black line) after irradiation (red line) and after heating the irradiated product at 60 °C for 15 mins (blue line).

The same process was executed for the photoproduct **1a-H⁺**. However, neither non-irradiated nor irradiated products contained organic radicles detectable by EPR spectroscopy (Fig. 5A). When **1b-H⁺** was analyzed by EPR spectroscopy a small derivative peak can be seen in the yellow-colored photo product, meaning a small concentration of radicals were detected (Fig. 5B). This result suggests that the **1a-H⁺** photoproduct utilizes

a mechanism that is different from both the methyl viologen and **1b-H⁺**. Our hypothesis is a nitrogen sulfur interaction is facilitated through a radicle intermediate which is silenced in the color changed state of **1a-H⁺**.

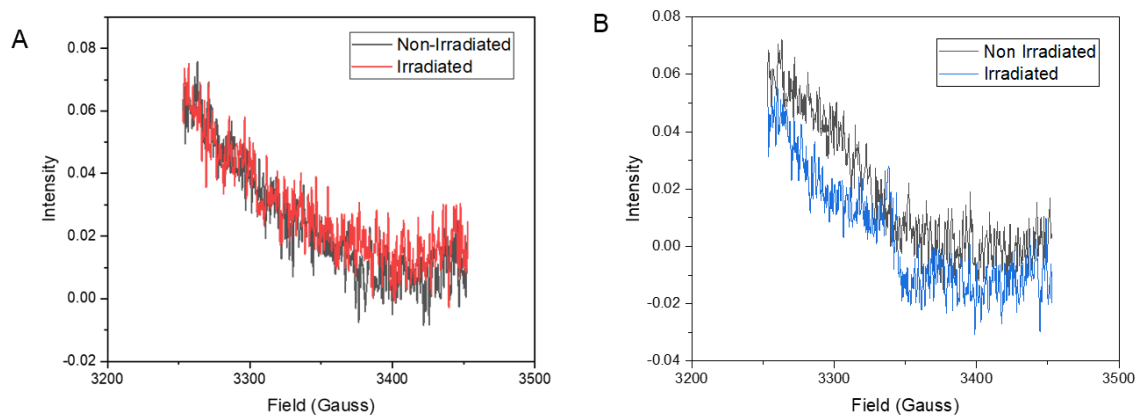


Figure 5. EPR spectra before and after irradiation of the solid A) **1a-H⁺** without the presence of any radicles and B) **1b-H⁺** shows the presence of a small radicle concentration.

Power X Ray diffraction was used to determine if there was a change in the unit cell of **1a-H⁺** after irradiation (Fig. 6).^{41,42} A significant change in peak intensity would indicate a change in atomic positions of within a lattice structure. A change in peak width would indicate a change in lattice strain. The formation of a new peak would suggest a new unit cell must be considered. The present XRD did not show any changes after irradiation; therefore, there is not a significant change in the crystal structure of **1a-H⁺** in the magenta state compared to the yellow state.

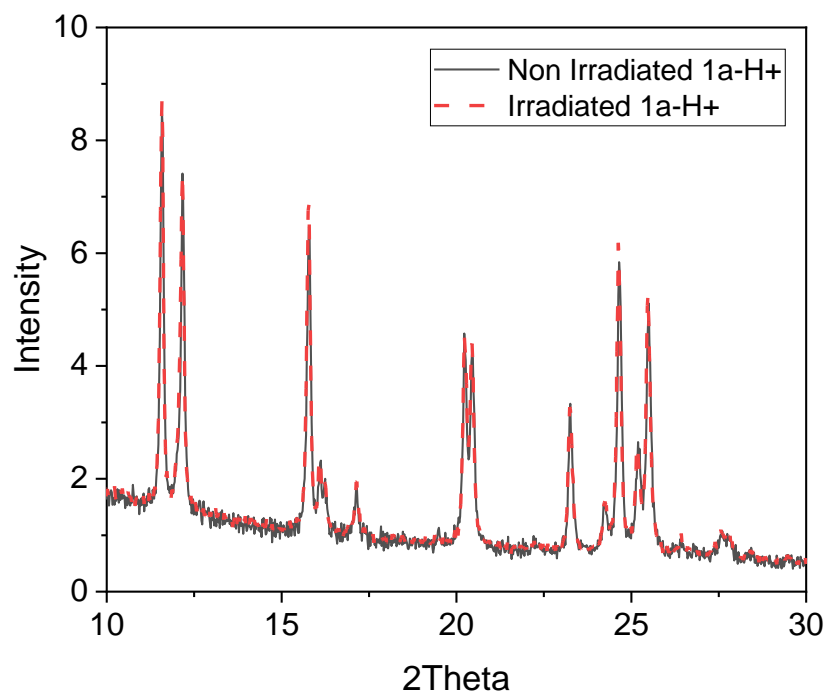


Figure 6. Powder XRD for 1a-H+ before irradiation (black solid line) vs irradiated 1a-H+ (red dashed line).

Other wavelengths of light within the visible range were observed to induce color change for the solid product (Fig. 7). All the wavelengths were emitted from a handheld UltraFire LED flashlight source (3 watts), to maintain consistent flux. Blue light (470 nm) irradiation was able to achieve color change to a similar intensity as 395 nm irradiation. As the wavelength increased the photoproduct changed color to a lesser degree. Green light (520 nm) had minimal color change and red light (630 nm) had no color change. This experimental result agrees with simulation data that will be discussed later.

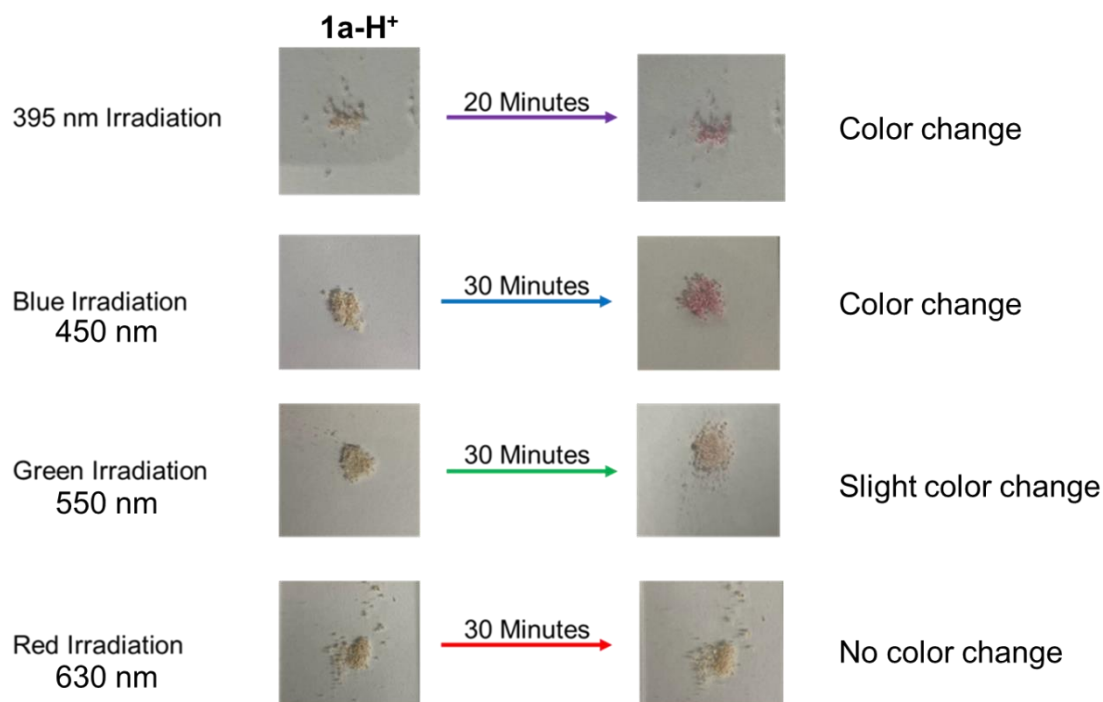


Figure 7. Irradiation of $1a-H^+$ with various wavelengths of visible light. Irradiation with 395 and 470 nm (blue) light induced significant color change while 520 nm (green) light induced slight color change to pink. Irradiation with 630 nm (red) light was unsuccessful at inducing color change.

2.3.2 Solution State Color Change

A photochromic response in solution state is key for investigating spectroscopic differences between the yellow and pink forms. An irreversible photochromic response is observed with $1a-H^+$ at concentrations ≥ 400 mM in polar aprotic solvents such as chloroform. Below 400 mM $1a-H^+$, the chloroform containing solution was permanently yellow colored and unaffected by UV light. In polar protic solvents such as methanol, $1a-H^+$ was permanently colored pink at all concentrations and unaffected by UV irradiation. Reversible photochromism was observed in glycol ether solvents including triethylene glycol monomethyl ether (TEGMME) and polyethylene glycol 300 g/mol. However, solubility of $1a-H^+$ in these solvents was poor. As a result, a 50:50 (v/v) mixture

of chloroform (CHCl_3) and TEGMME was the best solvent mixture for reversible photochromic response. This solvent system allowed for photochromic response for solutions as low as 20 mM (Fig. 8A).

After 2 minutes of 395 nm irradiation the 20 mM solution of **1a-H⁺** began to show color change. A main absorption band at 550 nm, which is responsible for the pink color, along shoulder peaks at 410 nm, 470 nm, 510 nm, and a broad absorption greater than 600 nm started to appear (Fig. 8B). The absorbance at 550 nm reached its maximum intensity after 20 minutes of irradiation. There was a slight decrease in absorbance following irradiation times exceeding 20 minutes, we attribute this to a thermal effect of prolonged light source usage. After heating the irradiated sample for 4 minutes at 75 °C the 550 nm peak returned to a similar absorbance exhibited in the non-irradiated state. The cyclability of the color change is shown by Figure 8C. The absorbance max remained consistent after 5 consecutive irradiations. The thermal treated state slightly increased with each cycle, but then plateaued after the fourth cycle. If allowed to rest in the dark for 18 hours, the irradiated sample was completely reversible back to the non-irradiated state, where all photo induced bands disappeared (Fig. 8D).

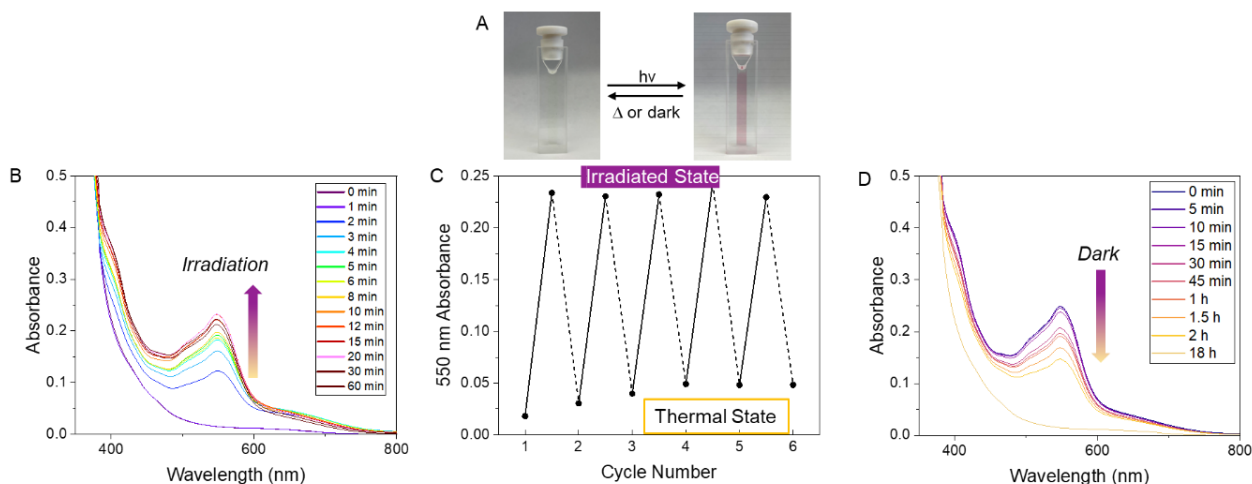


Figure 8. (A) Reversible color change of 20 mM **1a-H⁺** dissolved in CHCl₃:TEGMME 50:50 and its (B) absorption spectra under timed 395 nm irradiation. (C) Cyclability of photochromic response after heating for 4 minutes under 75 °C followed by 20 minutes of irradiation. (D) Decay of color after irradiated solution is left in dark storage over time.

Photochromism can take place at low concentrations when the solvent system contains a hydroxyl terminated oligomer such as TEGMME. However, photochromism is deactivated for a 20 mM solution of **1a-H⁺** when the solvent system is a 50:50 (v/v) mixture of triethylene glycol dimethyl ether (TEGDME) and CHCl₃ (Fig. 9A). A peak at 550 nm does not appear after 60 minutes of 395 nm irradiation. Yet absorbance at 450 nm continue to increase with irradiation time. When the solution concentration is increased to 80 mM photochromism returns (Fig. 9B). Here it is hypothesized that the hydroxyl group stabilizes the SO₂-bipyridine interaction, allowing for appreciable photo response at low chromophore concentration.

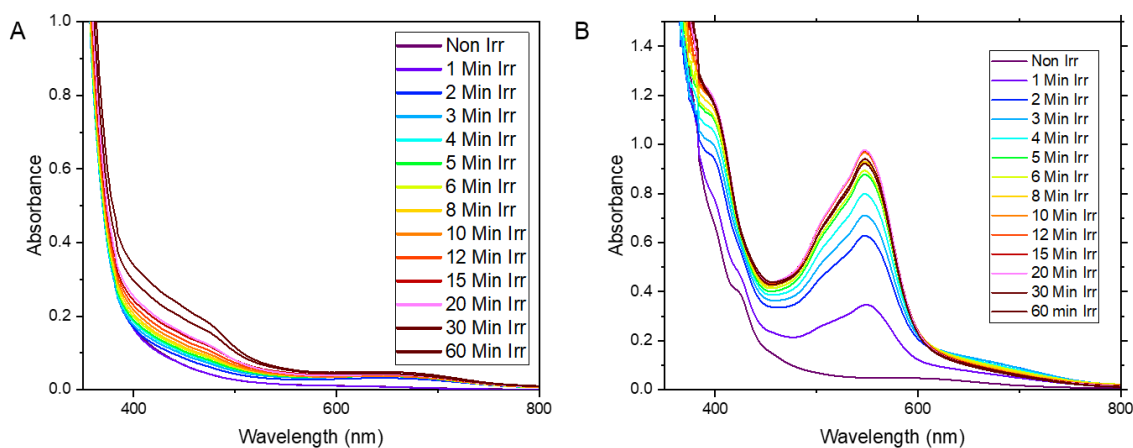


Figure 9. Photochromic response of $1a-H^+$ dissolved in $CHCl_3$:TEGDME 50:50 under timed 395 nm irradiation for a A) 20 mM solution and B) 80 mM solution.

2.3.4 Solution state SO_2 exposure

Direct SO_2 exposure to solutions of non-photochromic **1b** and **1b- H^+** provided further evidence for the cause of visible range absorptions. 20 mM solutions of **1b** and **1b- H^+** were dissolved in the 50:50 TEGMME: $CHCl_3$ solvent system and initially appeared clear. SO_2 bubbling was performed in the dark, and after 5 minutes of SO_2 exposure a color change from colorless to magenta occurred. The UV visible spectrum of the SO_2 saturated solutions appeared with identical absorbances to what was present in Figure 8B, a maximum absorbance at 550 nm with shoulder peaks at 410 nm, 470 nm, 510 nm, and a broad absorption greater than 600 nm (Fig. 10). Predictably, the same SO_2 saturation response was seen for solutions of **1a** and **1a- H^+** in the absence of light. Furthermore, unmodified 2,2'-bipyridine itself had a response to a SO_2 saturated solution with a λ_{max} absorbance at 525 nm. The shift to lower wavelength absorption is due to the decrease in conjugation without the presence of an ester. For all samples, 5 mins of SO_2 bubbling causes is a significant color change to magenta; however, 18 hours of equilibration results

in a more intense color. When compared to the UV activated pathway, which can achieve maximum absorbance in 20 minutes, the kinetics of the color change is very slow. Nevertheless, we can attribute the visible absorptions to the bipyridine-SO₂ complex.

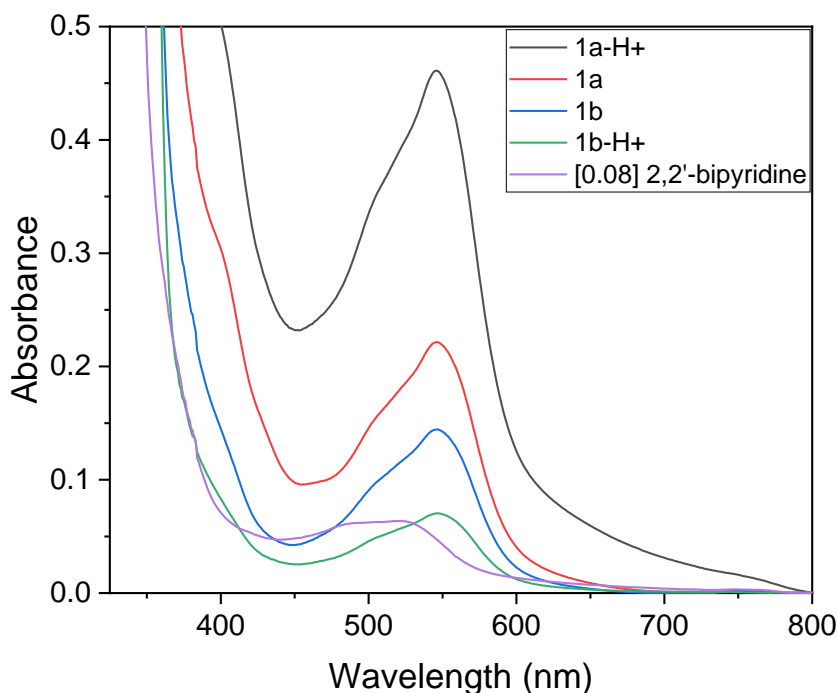


Figure 10. UV-vis absorption spectra of 20 mM 1a-H⁺ (black line), 20 mM 1a (red line), 20 mM 1b (blue line), 20 mM 1b-H⁺ (green line), 80 mM 2,2'-bipyridine (purple line) in 50:50 CHCl₃:TEGMME after 5 minutes of SO₂ bubbling followed by 18 hours of dark storage.

The color change from a yellow-colored solution containing protonated bipyridine to a magenta-colored solution saturated with SO₂ is accredited to the equilibrium between the bipyridine-SO₂ complex and bipyridinium. The small atomic size hydrogen atom is the preferred binding partner with the bipyridine nitrogen. In the presence of excess amounts of SO₂, the equilibrium will shift to the less favorable bipyridine-SO₂ complex, resulting in a color change to pink. Figure 11A shows several possible structures for bipyridine to

form in the presence of excess SO_2 . Upon addition of more HCl , the yellow color will prevail as bipyridinium is ultimately preferable.

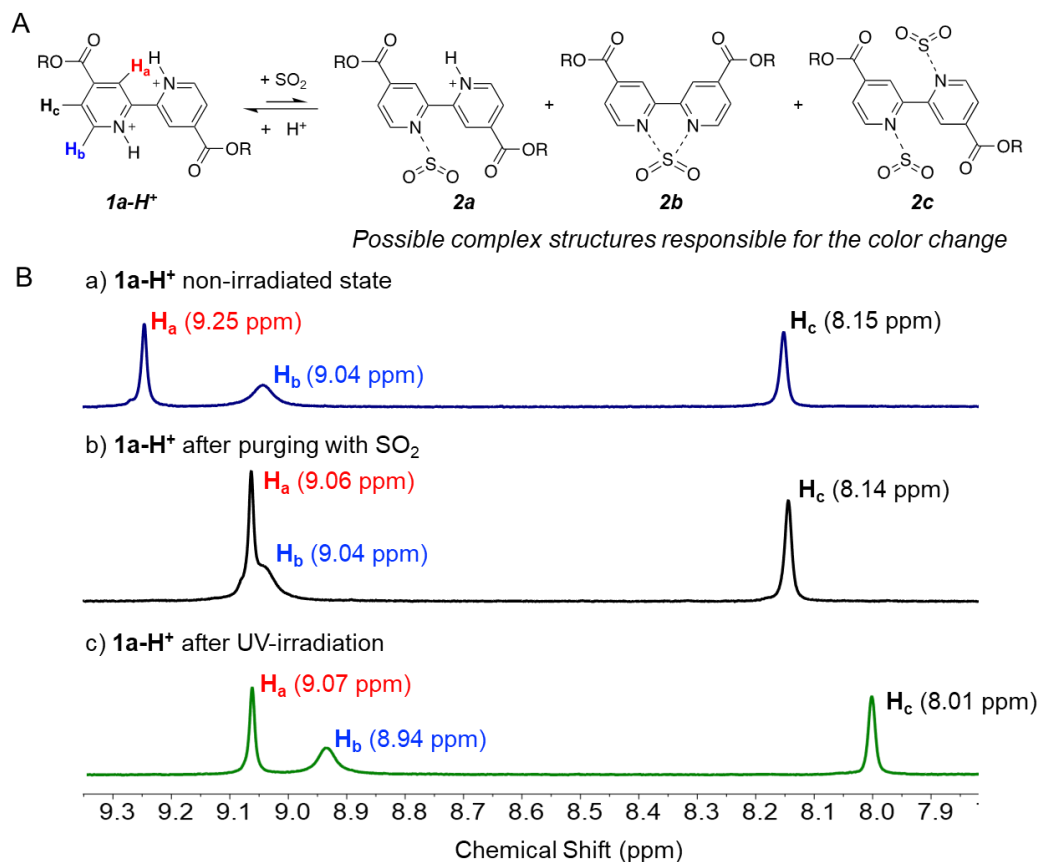


Figure 11. A) Equilibrium between the protonated bipyridyl and bipyridine- SO_2 complex. B) ^1H NMR shifts for a) non-irradiated $1\mathbf{a}\text{-H}^+$, b) $1\mathbf{a}\text{-H}^+$ after SO_2 bubbling in CDCl_3 , and c) $1\mathbf{a}\text{-H}^+$ irradiated with 395 nm light for 20 min in the solid state and then dissolved in CDCl_3 for data collection.

^1H NMR can be used to quantify the equilibrium between bipyridinium and bipyridine- SO_2 . After 3 minutes of bubbling HCl gas in a solution containing $1\mathbf{a}$ all aromatic protons shift downfield (Fig. 11B-a). The most downfield hydrogens are attached to the bipyridine ring at the 6,6'-positions (H_a). Due to the significant downfield shift, it was assumed that the bipyridine is diprotonated. After bubbling with SO_2 for 5 minutes H_a exhibited a significant upfield shift, while H_b and H_c remained unaffected (Fig. 11B-b).

An upfield shift signifies H_a is in a more electron-rich environment. The proximity of H_a to SO_2 in complex 2c would be consistent an upfield shift. Also considering that H_b and H_c were unaffected after SO_2 exposure, an exchange from a diprotonated bipyridinium to a 2:1 SO_2 :bipyridine complex could explain the spectra observed (Fig. 11B-b).

We then compared the NMR shifts seen in the SO_2 saturated solution to what is observed in the irradiated solid for **1a-H⁺** shown in Fig. 1. After irradiation in the solid state, followed by dissolution in $CDCl_3$, all three aromatic ring protons exhibited clear upfield shifts (Fig. 11B-c). The upfield shift of H_a identically matches what was observed in the SO_2 saturated solution. However, these changes are more likely due to deprotonation of bipyridine rather than formation of bipyridine- SO_2 complex, since the solution is yellow colored upon dissolution in $CDCl_3$ at NMR concentration (5 mg/mL or 14 mM). The color of the NMR solution indicated that bipyridine and SO_2 are dissociated upon dissolution. As a result, the NMR suggests a release of HCl upon UV irradiation in the solid state. However, it is possible that the formation of an SO_2 -bipyridine complex in the solid state could facilitate deprotonation, since similar trends were observed following the irradiation of nonphotochromic compounds **1b-H⁺** but to a significantly smaller extent (Fig. 12). Before use, **1a-H⁺** and **1b-H⁺** were sufficiently dried for 18 hours at 45 °C under vacuum, ruling out the loss of HCl has a thermal effect induced by the UV lamp.

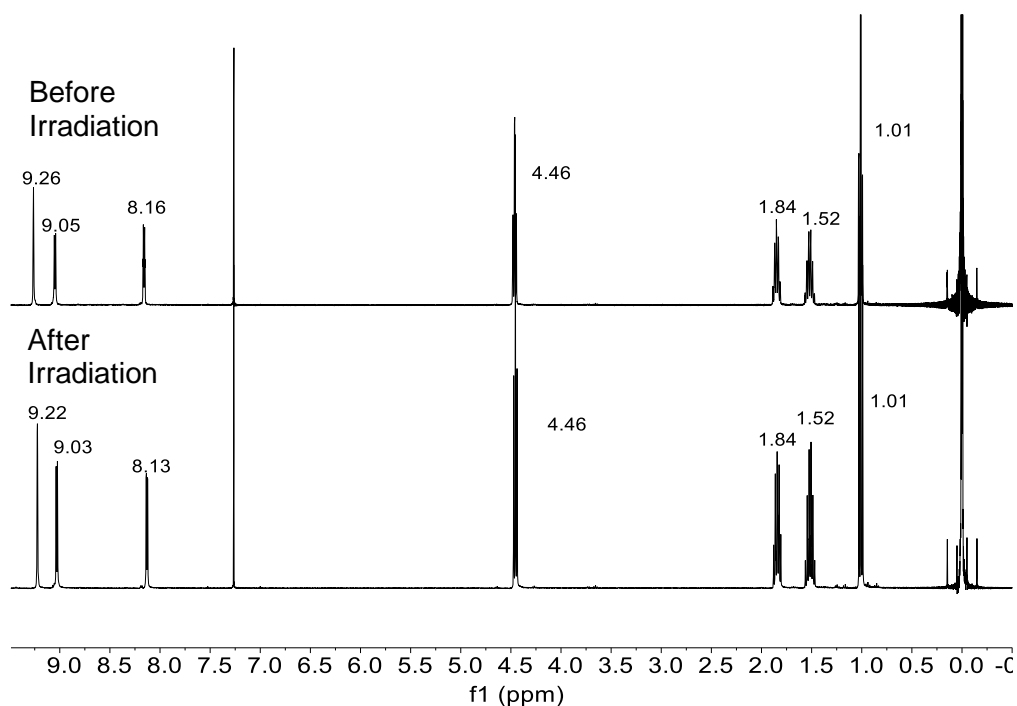


Figure 12. ^1H NMR shifts before and after 30 min irradiation at 395 nm for 1b-H^+ indicate a smaller loss of HCl upon irradiation for products that have never been exposed to SO_2 .

2.3.6. Solution state fluorescence.

During irradiation of a 20mM 1a-H^+ solution in 1:1 TEGMME: CHCl_3 fluorescence occurs. Excitation with 395 nm light emits a wavelength of 454 nm. Blue emitters are rare in literature especially for SO_2 containing compounds. Fluorescence of other wavelengths have been reported for SO_2 containing compounds.^{43–45} Interestingly, when the irradiation wavelength is shifted, the fluorescence wavelength also shifts to the same direction (Fig. 13A). The emitted 454 nm light is the highest intensity compared to other wavelengths of light emitted by excitations other than 395 nm (Fig. 13B). It was also noticed that when excited with 454 nm light, the wavelength of the blue emission, another weaker secondary emission occurs at 525 nm.

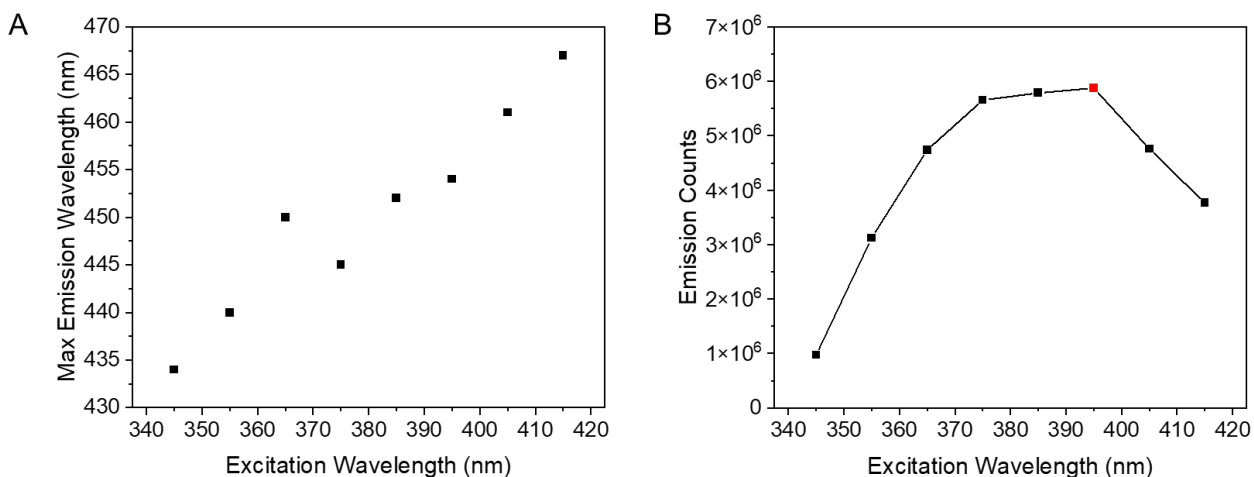


Figure 13. (A) A positive linear relationship between excitation wavelength and emission wavelength for 1a-H⁺ solutions containing TEGMME:CHCl₃ 50:50. (B) The emission of 454 nm light following 395 nm excitation (red point) is the highest intensity compared emissions induced by other excitation wavelengths.

3.2.7. Photoactivated mechanism and theoretical calculations

Thus far it is uncertain which of the complex structures (Fig. 11A 2a-2c) could be responsible for the charge transfer band present at 550 nm. To answer these questions, we collaborated with Dr. Samuel Odoh's lab to determine the optimized structures of complexes **2a-2c** before and after photo-irradiation through DFT calculations. The ground state equilibrium N-S bond distances were between 2.50-2.65 Å for **2a-2c**. These bond distances presented a calculated absorption spectra without a feature above 300 nm, consistent with our experimental results.

The potential energy surface of complexes 2a-2c, through constraining N-S distances, suggest a unique potential energy surface for **2b-cis** (Fig. 14, red line). It shows a local energetic minimum where the N-S distance is 1.662 Å. Without geometrical constraints, the structure with this N-S distance was also found to be optimal. Compared to the ground state equilibrium bond distance, this region lies 42.7-43.3 kcal/mol higher in energy. Therefore, light with wavelengths below 627 nm will populate this minimum. This was experimentally consistent with Figure 7 where exclusively red light (630 nm) did not induce color change for **1a-H⁺**.

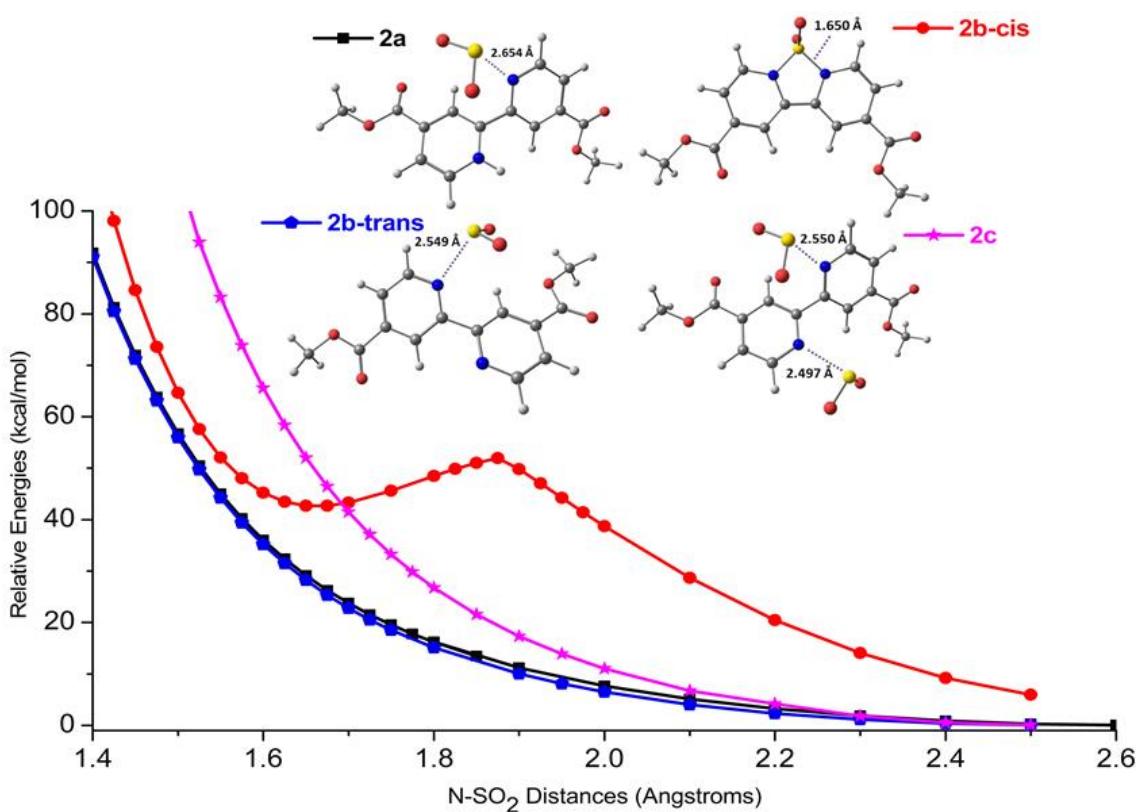


Figure 14. Structures and potential energy surfaces of **2a-2c** obtained at the B3LYP-D3BJ/def2-TZVP level. Structure 2a (black line) 2b-trans (blue line), and 2c (pink line) exhibit no unique features representative of a photochromic response, while 2b-cis (red line) shows a local energetic minimum at a decreased bond length of 1.662 Å

Light with wavelengths of 365-395 nm corresponds to photons with the energy of 72-78 kcal/mol. Upon irradiation with this wavelength the N-S distance of 1.475 Å is achieved for **2b-cis**. The calculated absorbance spectra for **2b-cis** at an N-S bond distance 1.475 Å (Fig. 15 green line) as well as the localized minimum bond distance of 1.662 Å (Fig. 15 red line) produced appreciable absorptions between 500 and 550 nm. Complex structures of **2a**, **2b-trans**, and **2c** did not produce significant peaks at their corresponding bond distances at 72-78 kcal/mol. The computation results indicate that photoirradiation results in a non-equilibrium shortened N-S distance. Upon 395 nm exposure the 1.475 Å N-S bond distance relaxes to the local minimum of 1.662 Å, which is responsible for the absorption near 550 nm.

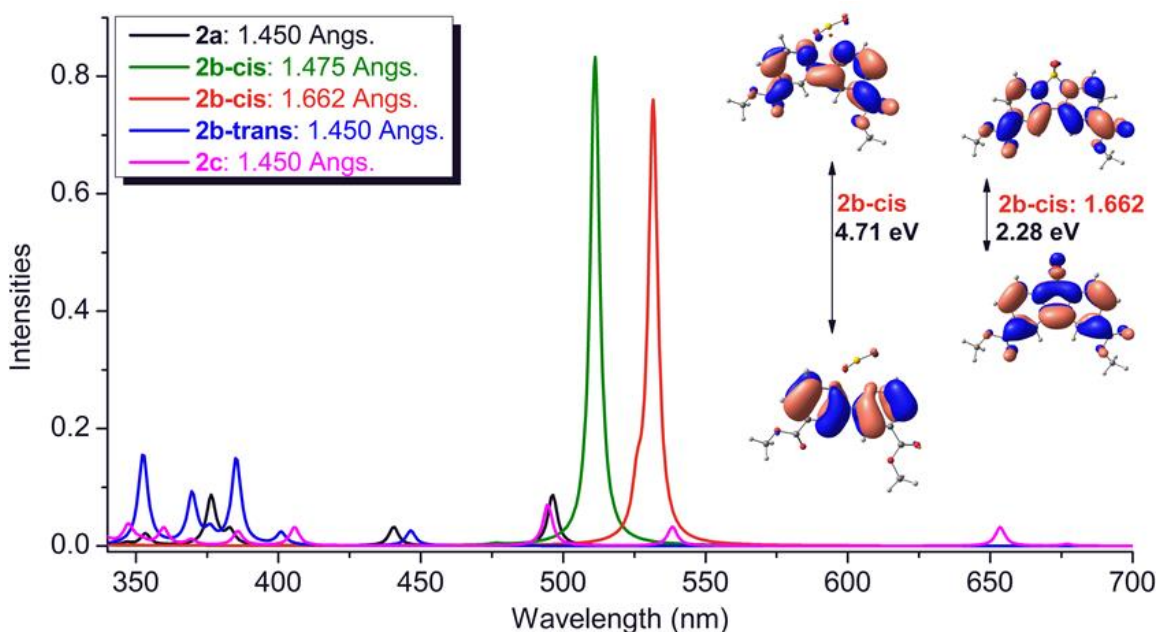


Figure 15. Calculated spectra of non-equilibrium structures of 2a-2c formed after photoirradiation. Spectra are convoluted with Lorentzian functions with FWHM of 4 nm. Spectra of 2b-cis conformations of N-S bond distances 1.475 Angs. (green) and 1.662 Angs. (red) contain absorptions between 500-550 nm, consistent with experimental results.

Through domain-based local pair natural orbital similarity transformed equation of motion-coupled cluster singles and doubles (STEOM-DLPNO-CCSD) calculations it was

determined that as SO₂ becomes closer to the bipyridine rings the highest occupied molecular orbital (HOMO) is significantly destabilized. This reduces the gap to the lowest unoccupied molecular orbital (LUMO) to 2.28 eV from 4.71 eV at equilibrium. This factor leads to the intense absorption at 500-550 nm at the local energetic minimum of **2b-cis**.

For simplicity, calculations were performed on 2,2'-bipyridine-4,4'-dimethyl ester substituents. Experimentally, changing dibutyl ester to a dimethyl ester product was no longer photoactive. However, a didecyl ester product was still photochromic. Dimethyl ester is crystalline at room temperature while dibutyl and didecyl esters are amorphous solids at room temperature. Thus, the loss of photochromism can be attributed to the lack of retained SO₂ in the crystalline solid.

2.4 Summary of findings

A synthesis was proposed for the formation of a photochromic small molecule 2,2'-bipyridine-4,4'-dibutyl ester (scheme 1, route a). This molecule undergoes a color change in the solid state from yellow to pink after minutes of 395 nm irradiation. The color change is stable in the dark and at elevated temperatures and is only reversible through exposure to acidic conditions. The color change mechanism was deemed unique from the well-known viologen after EPR analysis. A variation in the synthetic route (scheme 2, route b) produced an identical NMR spectrum, but no longer had photochromic response. Here we begin to attribute color change to an interaction between bipyridine and SO₂, a side product of the first synthesis route. IR analysis of the solid state 1a and 1b does not show any free SO₂ (1340 cm⁻¹); however, it did show two binding modes between 900-1020 cm⁻¹ which appeared exclusively in 1a.

Solution state spectroscopy required a unique solvent system for low concentration reversible photochromic response. The proposed solvent system was a 50:50 (v/v) chloroform to triethyl glycol monomethyl ether mixture. Using this solvent system, we were able to measure an absorbance at 550 nm which corresponds to the pink color. This peak reached a maximum intensity following 20 minutes of 395 nm irradiation. The 550 nm absorbance returned to the level of the non-irradiated state following 4 minutes of 75°C or 18 hours of dark storage. The color change was reversible over many cycles without loss of color intensity. Upon 395 nm irradiation the solution fluoresces blue light. To evaluate the mechanism of bipyridine SO₂ responsible for color change, a solution of non-photochromic **1b** was saturated with SO₂. This afforded a UV-vis spectra containing peaks like the irradiated **1a-H⁺** solution. Furthermore, ¹H NMR spectra exhibit similar shifts from the non-irradiated sample induced by irradiation or saturation with SO₂.

Density functional theory calculation data provided by Dr. Samuel Odoh's group evaluated the possible bipyridine-SO₂ complex structures (**2a-2c**) responsible for the absorption at 550 nm in chloroform. None of the suggested complexes had absorptions above 300 nm in the ground state; however, optimizing geometry through constrained N-S distances described 2b-cis to have a local minimum on the potential energy diagram at a bond distance of 1.662 Å. This local minimum required a wavelength below 627 nm overcome the energy barrier from the ground state. A N-S interaction constrained at this bond distance produced an absorption spectrum which had a unique feature at 532 nm, consistent with experimental observations.

Chapter 3. Application in photochromic polymers

3.1 Introduction

This chapter discusses the synthesis and photoresponsivity of polymers functionalized with the small molecule 2,2'-bipyridine-4,4'-diester. In a polymer matrix, it is known that photochromic transitions are generally slower compared to in solution. This is due to the lack of free volume which serves to restrict the segmental motion and increase steric hinderance in certain isomers.⁴⁶ Since the mechanism observed in the small molecule chromophore is induced by a shortening of a bipyridine-SO₂ bond distance, reduced molecular motion should not greatly effect photochromic response. However, SO₂ mobility is affected by the system polarity. The ability for SO₂ to interact with the chromophore within a polymer matrix is dependent on repeat unit character. When comparing two common polymers polyethylene and polypropylene, SO₂ can permeate through a polyethylene matrix at a rate 7 times faster than polypropylene.⁴⁷ Here we synthesized chromophore containing polymer derivatives of low and high molecular weights polyethylene glycol and polypropylene glycol. The photoresponsivity was shown to exhibit thermally reversible color change for both low and high molecular weights of polyethylene glycol. Yet only low molecular weight polypropylene glycol containing photopolymers are photochromic while high molecular weight was unresponsive. This suggests SO₂ mobility with a polar maxtrix as an important factor for polymer photoresponsivity.

Currently, other members in the Yang group are interested in the mechanoresponsivity of bipyridine containing polymers. Introductory experiments

regarding viscosity change before and after irradiation were analyzed. A small decrease in viscosity was identified after irradiation of the polymeric samples.

3.2 Experimental

3.2.1 Synthesis

2,2'-bipyridine 4,4'-dicarboxylic acid (0.637 g, 2.62 mmol), 10 mL of thionyl chloride, and 100 μ L pyridine was added to a 50 mL round bottom flask, and the mixture was refluxed for 48 hours in N₂ atmosphere. The yellow-colored 2,2'-bipyridine 4,4'-diacid chloride solution was heated under reduced pressure to remove thionyl chloride. Then for two iterations, chloroform was added to the yellow solid and subsequently removed under reduced pressure. The acid chloride intermediate was dissolved in 3 mL chloroform. Polymer chain extender of either PEG 300, 2000, or 4000 g/mol or PPG 425 or 4000 g/mol (2 equivalents) was dissolved in 2 mL chloroform and added dropwise into the acid chloride solution followed by the addition of 200 μ L pyridine. The mixture was stirred at room temperature for 18 hours in N₂ atmosphere.

3.2.2 Irradiation Procedure

An UltraFire 502UV LED flashlight (395 nm) was the primary irradiation source. The samples were irradiated at a distance 2.5 cm from the light source.

3.2.3 Viscosity measurements

Viscosity measurements were performed on a TA Instruments Discovery HR-2 Hybrid Rheometer. A parallel plate geometry with a 450 nm gap was filled and trimmed with 2,2'-bipyridine-4,4'-diester functionalized with PEG 300 g/mol. First, a flow sweep was performed from 10⁻¹ to 10² Hz to determine the yield stress of the product. The yield stress

was determined to be 10 Hz. Then to determine the viscosity of the sample, a flow peak hold was performed at the yield stress for 180 seconds taking a measurement every second. The reported viscosity is an average of the 180 measurements.

3.3 Photochromic response of polymer

Utilizing the small molecule chromophore 2,2'-bipyridine-4,4'-diester, photochromic polymers were obtained. We polymerized 2,2'-bipyridine-4,4'-dicarboxylic acid with polyethylene glycol (PEG) 2000 g/mol via acid chloride intermediate (Scheme 1, route a). The acid chloride intermediate provided SO₂ and HCl to allow for photochromic response. A polyether was chosen due to the success of glycol ether solvents to facilitate low concentration reversible photochromic response for small molecule solutions. The resulting polymeric product was a white semicrystalline solid. Upon irradiation with 395 nm light through a UV stencil, the white solid was able to turn magenta selectively within the stencil (Fig. 16). After irradiation, the magenta color was stable for 24 hours in the dark at room temperature. The entirety of the product was then exposed to additional 395 nm irradiation, resulting in a wholistic color change. After 75 °C thermal treatment for 4 minutes, the magenta-colored solid was converted to a white colored liquid which rapidly cooled back to a white semicrystalline solid. The white solid was also stable at room temperature in the dark but was readily able to color change to magenta upon additional UV irradiation. The stability of both the non-irradiated white solid and the irradiated pink solid at room temperature differentiates this material from many other photochromic systems.

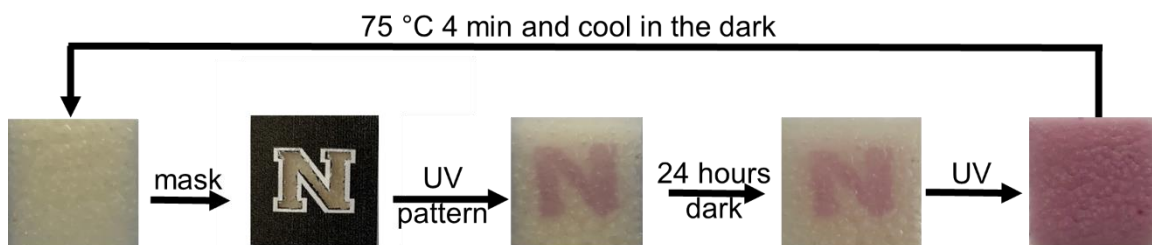


Figure 16. 2,2'-bipyridine-4,4' diester functionalized polyethylene glycol 2000 g/mol polymers showing stable photo-responses after irradiation, thermal treatment, and dark storage.

The stability of the magenta-colored irradiated state is the same as the small molecule solid, there is a lack of HCl in the solid state. Upon irradiation, the bipyridine-SO₂ interaction is stabilized and HCl diffuses into the PEG matrix. Only until the sample is in the liquid state can HCl diffuse back into the bipyridine moieties, which breaks the SO₂-bipyridine colored complex. The small molecule solid has a much higher melting point therefore the liquid state molecular mobility cannot be reached for reversible photochromic response.

More photochromic polymers composed of other molecular weights of PEG as well as polypropylene glycol (PPG) were synthesized and exhibit unique characteristics (Fig. 17). Polymers containing low molecular weight PEG 300 g/mol (Fig. 17 , 1)) and PPG 425 g/mol (Fig. 17 , 3)) exhibit similar properties for photochromic response. As synthesized, they are yellow viscous liquids that are stable in the dark at room temperature. Upon first irradiation with 395 nm UV light, the yellow liquid color changes to a red wine-colored liquid. This color is also stable in the dark at room temperature. If heated at 75 °C for 4 minutes the red color returns to yellow, but only at elevated temperatures. Upon cooling in

dark storage for 1 hour, the red color returns without need for additional irradiation. This color change relationship indicates a permanent change following the first irradiation

The photo-response of polymers containing higher molecular weight PEG and PPG 4000 g/mol are distinct from one another. The first difference is the phase of the two products as synthesized. The product containing PEG 4000 g/mol is solid at room temperature while PPG 4000 g/mol is liquid at room temperature. This is due to the increase in free volume by PPG's methyl group, which does not form an ordered solid at 4000 g/mol.⁴⁸ The PEG 4000 g/mol containing polymer responds identically to the PEG 2000 g/mol described earlier, but PPG 4000 is unresponsive to photoirradiation. This can be explained by polarity difference for PPG compared to PEG.⁴⁷ PEG is more polar which facilitates dispersion of SO₂ throughout the matrix affording color change for low chromophore concentrations. While using higher molecular weight polymers the concentration of bipyridine chromophores decrease, causing the mobility of SO₂ through the polymer matrix to play an important role. If there are not enough SO₂ molecules near the bipyridine moieties due to low distribution, then colored SO₂-bipyridine complexes cannot form.









	Polymer Used	Molecular Weight	Photochromism	Before 365 nm	After 365 nm
1	PEG	300	Yes		
2	PEG	4000	Yes		
3	PPG	425	Yes		
4	PPG	4000	No		

Figure 17. Photochromic response of 2,2'-bipyridine-4,4'-diester polymeric samples of type PEG 300 (1), PEG 4000 (2), PPG 425 (3), PPG 4000 (4)

3.4 Irradiation dependence on viscosity

Viscosity differences in the never irradiated state compared to the irradiated state evaluated using a parallel plate rheometry assembly. A sample containing a functionalized PEG 300 g/mol sample was used for this test (Fig. 18). Following the first irradiation a slight decrease in viscosity occurs. Thermal treatment of the irradiated form followed by sufficient cooling causes an increase of viscosity greater than twice of the never irradiated product. A second irradiation of the polymer again results in a viscosity decrease. A viscosity decrease is indicative of fewer intermolecular attractive interactions occurring in the irradiated state.⁴⁹ This trend is consistent with the increase in electron density signified by an NMR upfield shift following irradiation of photochromic the small molecule (Fig. 10). The increase of electron density on the will likely repel two bipyridine moieties from

one another due to Coulomb's law.⁵⁰ The repulsion of the bipyridine moieties will induce less PEG chain entanglement thereby resulting in a lower viscosity liquid.

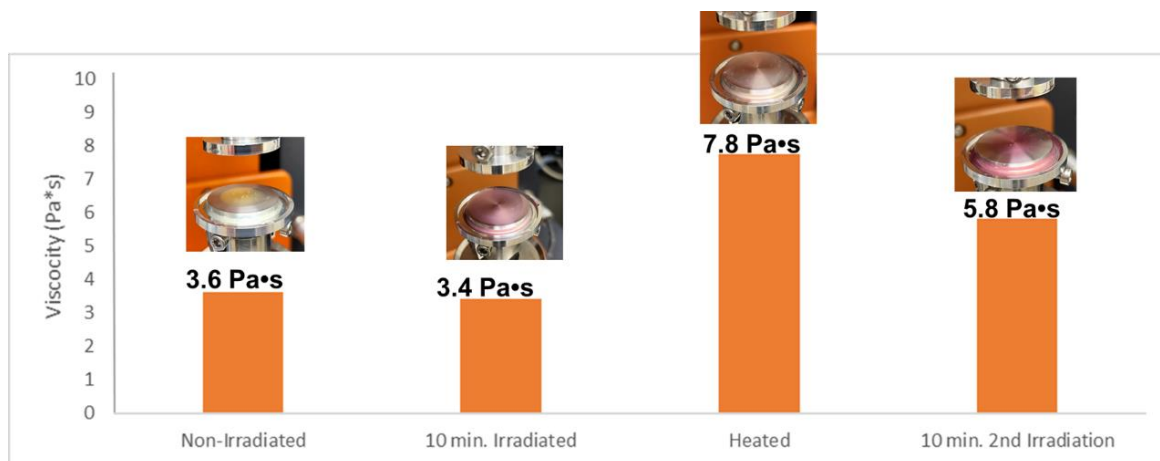


Figure 18. Viscosity response of 2,2'-bipyridine 4,4'-diester containing polyethylene glycol 300 g/mol in the irradiated and non-irradiated states.

3.5 Summary of Findings

Polymers functionalized with 2,2'-bipyridine-4,4'-diester in the backbone were synthesized using the same synthetic route (a) as the photochromic small molecule. The photochromic response is tunable based on what backbone is used and at what molecular weight. Polyethylene glycol (PEG) 300 g/mol and polypropylene glycol (PPG) 425 g/mol backbones are similar in response as they are yellow liquids that are color stable until the first direct irradiation. Upon irradiation they color change to a red liquid that is reversible back to the yellow state under 75 °C heat. Upon cooling to room temperature the red color begins to return to full intensity after 1 hour of dark storage. Furthermore, the viscosity of a PEG 300 g/mol was shown to decrease upon irradiation.

PEG 2000 and 4000 g/mol backbones yielded white semicrystalline solids that can color change to a pink solid upon direct UV irradiation. These samples are reversible after

4 minutes of heat back to the non-irradiated white solid. The white solid is stable for prolonged dark storage but can readily color change again with additional irradiation. PPG 4000 g/mol backbones were found to be non-photochromic.

Chapter 4. Conclusion and Outlook

4.1 Conclusions

A photochromic molecule containing 2,2'-bipyridine-4,4'-diester was synthesized as a small molecule product. Through spectroscopic analysis of two synthetic routes of the small molecule, in conjunction with computational data, the photochromic mechanism was predicted to involve a bipyridine-SO₂ charge transfer complex. Upon UV irradiation the N-S bond strengthens, which lowers the energy of the charge transfer band into the visible range. Reversible color change was found for a small molecule solution. After irradiation induced color change, a colored solution was reversible back to the non-irradiated state by dark storage or thermal treatment. It was demonstrated that color intensity remained consistent after many cycles of irradiation following thermal treatment. Polymers functionalized with 2,2'-bipyridine-4,4'-diester in the backbone demonstrated unique photochromic behavior depending on the backbone polarity and molecular weight.

4.2 Outlook

Future studies utilizing the present chromophore should focus on its photo-response as a polymer. Currently, a photochromic response has only been reported for linear chains. Given that the proposed mechanism is not reliant on significant molecular movement, it is hypothesized that crosslinked polymer networks should exhibit photochromic response. Formation of a crosslinked polymer network would allow for use as a photochromic thin

film and coating. Future work will focus on the mechanoresponsivity of bipyridine polymers. Considering how the viscosity decreased upon irradiation for linear polymers, it is hypothesized that the tensile strength of a photochromic film will also be affected by irradiation.^{51,52}

The SO₂ was the only tested Lewis acid in this study. SO₂ is considered a 'borderline Lewis acid' whose strength lies between a soft and hard acid. The photo response of other non-metal hard Lewis acids such as CO₂, and BF₃ or soft Lewis acids such as BH₃ or Br₂ may change the photoresponsivity. Selenium oxides will also be considered. Different Lewis acids would have unique charge transfer band absorbances, which could allow for photochromic response of many different colors.⁵³ Another approach is to vary the substituents on the bipyridines from electron-withdrawing to electron-donating groups.

Purging nitrogen gas limits the reaction's exposure to ambient air. The synthesis of the photo-responsive small molecule and polymer was completed only under nitrogen purge of the reaction vessel headspace, but not the reacting solution itself. Purging the reacting solution with inert gas would limit the oxidation of SO₂ to sulfur trioxide (SO₃) in air. Amine-SO₃ complexes have been widely reported in literature, therefore we plan to explore this interaction as what could drive the photo-response.^{54,55} Further oxidation states of sulfur oxides, such as SO₄²⁻, may also be considered for their role in the photo-response.

Quantitative evidence for the dissociation energy of the N-S bond could be performed through variable temperature infrared spectroscopy (VTIR).⁵⁶ These tests can precisely determine the strength of solid-gas interactions. The thermal treatment to force

reversible photo-response described in our work (75 °C for 4 minutes) was in excess of the minimum amount of energy necessary. A VTIR experiment would allow the stability of our described N-S interaction to be comparable to other reported N-S interactions in literature, which could enhance the novelty of what we observe. The dissociation energy can be extrapolated to determine a wavelength of light which can cause color change reversibility.

Conflicts of interest

None

References

- (1) Trommsdorff, H. Ueber Santonin. *Ann. der Pharm.* **1834**, *11* (2), 190–207.
- (2) Natarajan, A.; Tsai, C. K.; Khan, S. I.; McCarren, P.; Houk, K. N.; Garcia-Garibay, M. A. The Photoarrangement of α -Santonin Is a Single-Crystal-to-Single-Crystal Reaction: A Long Kept Secret in Solid-State Organic Chemistry Revealed. *J. Am. Chem. Soc.* **2007**, *129* (32), 9846–9847.
- (3) Zhuang, Y.; Ren, X.; Che, X.; Liu, S.; Huang, W.; Zhao, Q. Organic Photoresponsive Materials for Information Storage: A Review. *Adv. Photonics* **2020**, *3* (1), 14001.
- (4) Ercole, F.; Davis, T. P.; Evans, R. A. Photo-Responsive Systems and Biomaterials: Photochromic Polymers, Light-Triggered Self-Assembly, Surface Modification, Fluorescence Modulation and Beyond. *Polym. Chem.* **2010**, *1* (1), 37–54.
- (5) Zhang, J.; Zou, Q.; Tian, H. Photochromic Materials: More than Meets the Eye. *Adv. Mater.* **2013**, *25* (3), 378–399.
- (6) Liu, H.; Fan, Y.; Li, X.; Gao, K.; Li, H.; Yang, Y.; Meng, X.; Wu, J.; Hou, H. Photochromism of Metal–Organic Frameworks Based on Carbazole-Dicarboxylic Acid and Bipyridine: Sensing Adjustment by Controlling Strut-to-Strut Energy Transfer. *Dalt. Trans.* **2020**, *49* (23), 7952–7958.
- (7) Wojtecki, R. J.; Meador, M. A.; Rowan, S. J. Using the Dynamic Bond to Access Macroscopically Responsive Structurally Dynamic Polymers. *Nat. Mater.* **2011**, *10* (1), 14–27. <https://doi.org/10.1038/nmat2891>.
- (8) Irie, M.; Fukaminato, T.; Matsuda, K.; Kobatake, S. Photochromism of Diarylethene Molecules and Crystals: Memories, Switches, and Actuators. *Chem. Rev.* **2014**, *114* (24), 12174–12277.
- (9) Land, E. H. Experiments in Color Vision. *Sci. Am.* **1959**, *200* (5), 84–99.
- (10) Hartley, G. S. The Cis-Form of Azobenzene. *Nature* **1937**, *140* (3537), 281.
- (11) Berkovic, G.; Krongauz, V.; Weiss, V. Spiropyran and Spirooxazines for Memories and Switches. *Chem. Rev.* **2000**, *100* (5), 1741–1754.
- (12) Tian, H.; Yang, S. Recent Progresses on Diarylethene Based Photochromic Switches. *Chem. Soc. Rev.* **2004**, *33* (2), 85–97.
- (13) Bruin, F.; Heineken, F. W.; Bruin, M.; Zahlan, A. ESR Spectrum of the 4, 4'-Dipyridyl Radical. *J. Chem. Phys.* **1962**, *36* (10), 2783–2785.

- (14) Zeng, S.; Jiang, X.; Su, B.; Nan, X. China's SO₂ Shadow Prices and Environmental Technical Efficiency at the Province Level. *Int. Rev. Econ. Financ.* **2018**, *57*, 86–102.
- (15) Andres, R. J.; Kasgnoc, A. D. A Time-averaged Inventory of Subaerial Volcanic Sulfur Emissions. *J. Geophys. Res. Atmos.* **1998**, *103* (D19), 25251–25261.
- (16) Fioletov, V. E.; McLinden, C. A.; Krotkov, N.; Yang, K.; Loyola, D. G.; Valks, P.; Theys, N.; Van Roozendaal, M.; Nowlan, C. R.; Chance, K. Application of OMI, SCIAMACHY, and GOME-2 Satellite SO₂ Retrievals for Detection of Large Emission Sources. *J. Geophys. Res. Atmos.* **2013**, *118* (19), 11–399.
- (17) Srivastava, R. K.; Jozewicz, W.; Singer, C. SO₂ Scrubbing Technologies: A Review. *Environ. Prog.* **2001**, *20* (4), 219–228.
- (18) Quattrucci, E.; Masci, V. Nutritional Aspects of Food Preservatives. *Food Addit. Contam.* **1992**, *9* (5), 515–525.
- (19) Joksimovic, N.; Spasovski, G.; Joksimovic, V.; Andreevski, V.; Zuccari, C.; Omini, C. F. Efficacy and Tolerability of Hyaluronic Acid, Tea Tree Oil and Methyl-Sulfonyl-Methane in a New Gel Medical Device for Treatment of Haemorrhoids in a Double-Blind, Placebo-Controlled Clinical Trial. *Updates Surg.* **2012**, *64* (3), 195–201.
- (20) Aranthady, C.; Jangid, T.; Gupta, K.; Mishra, A. K.; Kaushik, S. D.; Siruguri, V.; Rao, G. M.; Shanbhag, G. V.; Sundaram, N. G. Selective SO₂ Detection at Low Concentration by Ca Substituted LaFeO₃ Chemiresistive Gas Sensor: A Comparative Study of LaFeO₃ Pellet vs Thin Film. *Sensors Actuators B Chem.* **2021**, *329*, 129211.
- (21) Ingle, N.; Mane, S.; Sayyad, P.; Bodkhe, G.; AL-Gahouari, T.; Mahadik, M.; Shirsat, S.; Shirsat, M. D. Sulfur Dioxide (SO₂) Detection Using Composite of Nickel Benzene Carboxylic (Ni3BTC₂) and OH-Functionalized Single Walled Carbon Nanotubes (OH-SWNTs). *Front. Mater.* **2020**, *7*, 93.
- (22) Khan, M. A. H.; Thomson, B.; Yu, J.; Debnath, R.; Motayed, A.; Rao, M. V. Scalable Metal Oxide Functionalized GaN Nanowire for Precise SO₂ Detection. *Sensors Actuators B Chem.* **2020**, *318*, 128223.
- (23) Nguyen, B.; Emmett, E. J.; Willis, M. C. Palladium-Catalyzed Aminosulfonylation of Aryl Halides. *J. Am. Chem. Soc.* **2010**, *132* (46), 16372–16373.
- (24) Deeming, A. S.; Emmett, E. J.; Richards-Taylor, C. S.; Willis, M. C. Rediscovering the Chemistry of Sulfur Dioxide: New Developments in Synthesis and Catalysis. *Synthesis (Stuttg.)* **2014**, *46* (20), 2701–2710.
- (25) Keller, J. W. Sulfur Dioxide–Pyridine Dimer. FTIR and Theoretical Evidence for a Low-Symmetry Structure. *J. Phys. Chem. A* **2015**, *119* (41), 10390–10398.

- (26) Kaes, C.; Katz, A.; Hosseini, M. W. Bipyridine: The Most Widely Used Ligand. A Review of Molecules Comprising at Least Two 2, 2'-Bipyridine Units. *Chem. Rev.* **2000**, *100* (10), 3553–3590.
- (27) Chen, F.; Wang, Y.-M.; Guo, W.; Yin, X.-B. Color-Tunable Lanthanide Metal–Organic Framework Gels. *Chem. Sci.* **2019**, *10* (6), 1644–1650.
- (28) Ai, Y.; Li, Y.; Fu, H. L.; Chan, A. K.; Yam, V. W. Aggregation and Tunable Color Emission Behaviors of L-Glutamine-Derived Platinum (II) Bipyridine Complexes by Hydrogen-Bonding, π - π Stacking and Metal–Metal Interactions. *Chem. Eur. J.* **2019**, *25* (20), 5251–5258.
- (29) Wei, S.; Lu, W.; Le, X.; Ma, C.; Lin, H.; Wu, B.; Zhang, J.; Theato, P.; Chen, T. Bioinspired Synergistic Fluorescence-Color-Switchable Polymeric Hydrogel Actuators. *Angew. Chemie* **2019**, *131* (45), 16389–16397.
- (30) Tan, H.; Lyu, Q.; Xie, Z.; Li, M.; Wang, K.; Wang, K.; Xiong, B.; Zhang, L.; Zhu, J. Metallosupramolecular Photonic Elastomers with Self-healing Capability and Angle-independent Color. *Adv. Mater.* **2019**, *31* (6), 1805496.
- (31) Hill, A. E. Reaction of Amines with Sulfur Dioxide. I. Aniline and Sulfur Dioxide. *J. Am. Chem. Soc.* **1931**, *53* (7), 2598–2608.
- (32) Faria, D. L. A.; Santos, P. S. Raman and Infrared Spectra of Some Aromatic Amine–Sulphur Dioxide Molecular Complexes. *J. Raman Spectrosc.* **1988**, *19* (7), 471–478.
- (33) Monezi, N. M.; Borin, A. C.; Santos, P. S.; Ando, R. A. The Thermochromic Behavior of Aromatic Amine-SO₂ Charge Transfer Complexes. *Spectrochim. Acta Part A Mol. Biomol. Spectrosc.* **2017**, *173*, 462–467.
- (34) Lee, P. C.; Schmidt, K.; Gordon, S.; Meisel, D. Resonance Raman of Viologen Radicals. *Chem. Phys. Lett.* **1981**, *80* (2), 242–247.
- (35) Kan, W.-Q.; Wen, S.-Z.; He, Y.-C.; Xu, C.-Y. Viologen-Based Photochromic Coordination Polymers for Inkless and Erasable Prints. *Inorg. Chem.* **2017**, *56* (24), 14926–14935.
- (36) Geraskina, M. R.; Dutton, A. S.; Juetten, M. J.; Wood, S. A.; Winter, A. H. The Viologen Cation Radical Pimer: A Case of Dispersion-Driven Bonding. *Angew. Chemie* **2017**, *129* (32), 9563–9567.
- (37) Martinez, C. R.; Iverson, B. L. Rethinking the Term “Pi-Stacking.” *Chem. Sci.* **2012**, *3* (7), 2191–2201.
- (38) Krishnan, C. V; Creutz, C.; Schwarz, H. A.; Sutin, N. Reduction Potentials for 2, 2'-Bipyridine and 1, 10-Phenanthroline Couples in Aqueous Solutions. *J. Am. Chem. Soc.* **1983**, *105* (17), 5617–5623.
- (39) Gero, A.; Markham, J. J. Studies on Pyridines: I. The Basicity of Pyridine Bases. *J.*

Org. Chem. **1951**, *16* (12), 1835–1838.

- (40) Chang, C. C. Infrared Studies of SO₂ on γ -Alumina. *J. Catal.* **1978**, *53* (3), 374–385.
- (41) Metzroth, T.; Hoffmann, A.; Martín-Rapún, R.; Smulders, M. M. J.; Pieterse, K.; Palmans, A. R. A.; Vekemans, J. A. J. M.; Meijer, E. W.; Spiess, H. W.; Gauss, J. Unravelling the Fine Structure of Stacked Bipyridine Diamine-Derived C 3-Disotics as Determined by X-Ray Diffraction, Quantum-Chemical Calculations, Fast-MAS NMR and CD Spectroscopy. *Chem. Sci.* **2011**, *2* (1), 69–76.
- (42) Harada, J.; Nakajima, R.; Ogawa, K. X-Ray Diffraction Analysis of Photochromic Reaction of Fulgides: Crystalline State Reaction Induced by Two-Photon Excitation. *J. Am. Chem. Soc.* **2008**, *130* (22), 7085–7091.
- (43) Mettee, H. D. Fluorescence and Phosphorescence of SO₂ Vapor. *J. Chem. Phys.* **1968**, *49* (4), 1784–1793.
- (44) Zhang, X.; Chen, J.-X.; Wang, K.; Shi, Y.-Z.; Fan, X.-C.; Zhang, S.-L.; Wu, L.; Li, Y.-Q.; Ou, X.-M.; Zhang, X.-H. Charge-Transfer Transition Regulation of Thermally Activated Delayed Fluorescence Emitters by Changing the Valence of Sulfur Atoms. *J. Mater. Chem. C* **2020**, *8* (48), 17457–17463.
- (45) Weng, W.; Aldén, M.; Li, Z. Quantitative SO₂ Detection in Combustion Environments Using Broad Band Ultraviolet Absorption and Laser-Induced Fluorescence. *Anal. Chem.* **2019**, *91* (16), 10849–10855.
- (46) Such, G.; Evans, R. A.; Yee, L. H.; Davis, T. P. Factors Influencing Photochromism of Spiro-Compounds within Polymeric Matrices. *J. Macromol. Sci. Part C Polym. Rev.* **2003**, *43* (4), 547–579.
- (47) Davis, E. G.; Rooney, M. L.; Larkins, P. L. Permeability of Polymer Films to Sulfur Dioxide at Low Concentration. *J. Appl. Polym. Sci.* **1975**, *19* (7), 1829–1835.
- (48) Rozanski, A.; Krajenta, A.; Idczak, R.; Galeski, A. Physical State of the Amorphous Phase of Polypropylene-influence on Free Volume and Cavitation Phenomenon. *J. Polym. Sci. Part B Polym. Phys.* **2016**, *54* (5), 531–543.
- (49) Yadav, S.; Shire, S. J.; Kalonia, D. S. Viscosity Behavior of High-Concentration Monoclonal Antibody Solutions: Correlation with Interaction Parameter and Electroviscous Effects. *J. Pharm. Sci.* **2012**, *101* (3), 998–1011.
- (50) Doblhofer, K.; Vorotyntsev, M. The Membrane Properties of Electroactive Polymer Films. In *Electroactive polymer electrochemistry*; Springer, 1994; pp 375–442.
- (51) Tong, Z.-Z.; Xue, J.-Q.; Wang, R.-Y.; Huang, J.; Xu, J.-T.; Fan, Z.-Q. Hierarchical Self-Assembly, Photo-Responsive Phase Behavior and Variable Tensile Property of Azobenzene-Containing ABA Triblock Copolymers. *Rsc Adv.* **2015**, *5* (6), 4030–

4040.

- (52) Ikejiri, S.; Takashima, Y.; Osaki, M.; Yamaguchi, H.; Harada, A. Solvent-Free Photoresponsive Artificial Muscles Rapidly Driven by Molecular Machines. *J. Am. Chem. Soc.* **2018**, *140* (49), 17308–17315.
- (53) Zalar, P.; Henson, Z. B.; Welch, G. C.; Bazan, G. C.; Nguyen, T. Color Tuning in Polymer Light-Emitting Diodes with Lewis Acids. *Angew. Chemie* **2012**, *124* (30), 7613–7616.
- (54) Moede, J. A.; Curran, C. Dielectric Properties and Ultraviolet Absorption Spectra of Addition Compounds of Sulfur Dioxide and Sulfur Trioxide with Tertiary Amines. *J. Am. Chem. Soc.* **1949**, *71* (3), 852–858.
- (55) Ahirrao, V.; Jadhav, R.; More, K.; Kale, R.; Rane, V.; Kilbile, J.; Raeq, M.; Yeole, R. An Accurate and Precise Analytical Method for Estimation of Active Sulfur Trioxide and Sulfuric Acid in Triethylamine Sulfur Trioxide Complex. *Asian J. Pharm. Anal.* **2022**, *12* (1).
- (56) Garrone, E.; Areán, C. O. Variable Temperature Infrared Spectroscopy: A Convenient Tool for Studying the Thermodynamics of Weak Solid–Gas Interactions. *Chem. Soc. Rev.* **2005**, *34* (10), 846–857.